Measurements of ^{31}S energy levels and reevaluation of the thermonuclear resonant ^{30}P$(p,\gamma)^{31}$S reaction rate

C. Wrede,[1,2,*] J. A. Caggiano,[3,†] J. A. Clark,[1,‡] C. M. Deibel,[1,‡] A. Parikh,[1,§] and P. D. Parker[1]
[1]*Wright Nuclear Structure Laboratory, Yale University, New Haven, Connecticut 06520, USA*
[2]*Department of Physics, University of Washington, Seattle, Washington 98195, USA*
[3]*TRIUMF, Vancouver, British Columbia V6T 2A3, Canada*
(Received 21 December 2008; published 10 April 2009)

By measuring the ^{31}P(^{3}He, t)^{31}S, ^{31}P(^{3}He, t)^{31}S$^*(p)^{30}$P, and ^{32}S$(d,t)^{31}$S reactions, the level scheme of ^{31}S has been refined and extended up to $E_x = 9.5$ MeV. A total of 17 new levels, and 5 tentative new levels, have been measured. In addition, 5 tentatively known levels have been confirmed. The uncertainties in the excitation energies of many known ^{31}S levels have been reduced substantially. Spin constraints have been made for 8 proton-unbound levels by measuring 18 triton-proton angular correlations from the ^{31}P(^{3}He, t)^{31}S$^*(p)^{30}$P reaction. Finite proton-decay branching ratios (including discrimination between decays to the ground state and first two excited states of ^{30}P) have been measured for 38 levels, and upper limits have been set for 3 additional levels. The lowest isospin $T = 3/2$ level has been observed, and candidates for the second and third $T = 3/2$ levels have been identified. The new experimental information on ^{30}P $+ p$ resonance parameters has been used together with data from previous measurements to calculate the thermonuclear, resonant ^{30}P$(p,\gamma)^{31}$S reaction rate over three orders of magnitude in temperature: $0.01 < T < 10$ GK. Good agreement is found with estimates based on Hauser-Feshbach statistical models over the range $0.08 < T < 10$ GK, but differences are found with rates previously estimated using the experimental information at hand.

DOI: 10.1103/PhysRevC.79.045803 PACS number(s): 26.30.−k, 26.50.+x, 25.55.Kr, 27.30.+t

I. INTRODUCTION

The thermonuclear ^{30}P$(p,\gamma)^{31}$S reaction rate is used in models of several astrophysical scenarios. It has been recognized to play an important role in determining the nucleosynthetic flow through the mass region $30 < A < 40$ at the peak temperatures $0.10 \leqslant T \leqslant 0.35$ GK of oxygen-neon (ONe) novae [1–3], and in the identification of presolar grains that may be of ONe nova origin [4–6]. At higher temperatures this reaction rate is an input to astrophysical models of *rp*-process nucleosynthesis sites: for example type I x-ray bursts ($T \lesssim 2$ GK). The rate of the inverse ^{31}S$(\gamma,p)^{30}$P photodisintegration reaction is determined directly from the forward rate. It is used to determine the magnitude of the ^{16}O(^{16}O, n)^{31}S$(\gamma,p)^{30}$P branch [7,8] in models of massive stars undergoing quiescent oxygen burning at temperatures up to 2.7 GK, and in models of the oxygen-neon layer of type II supernovae undergoing explosive oxygen burning at temperatures up to 4 GK. Until recently, the only available thermonuclear rates for the ^{30}P$(p,\gamma)^{31}$S reaction have been based on Hauser-Feshbach (HF) statistical models (e.g., [9–12]) that may not be reliable for nuclei as light and proton rich as ^{31}S due to the relatively low density of states immediately above the proton-emission threshold—particularly at the relatively low temperatures of novae [2]. An accurate experimental determination of the ^{30}P$(p,\gamma)^{31}$S reaction rate is thus crucial to the understanding of nucleosynthesis in massive ONe novae, contributes to the understanding of nucleosynthesis in a variety of other stellar environments/events, and may be used to test the accuracy of reaction rates based on HF models in this mass region.

The thermonuclear ^{30}P$(p,\gamma)^{31}$S reaction rate $N_A\langle\sigma\upsilon\rangle$, at temperature T, is expected to be dominated by the sum of contributions from narrow, isolated resonances r,

$$N_A\langle\sigma\upsilon\rangle = N_A\left(\frac{2\pi}{\mu kT}\right)^{3/2}\hbar^2\sum_r(\omega\gamma)_r e^{-E_r/kT}, \qquad (1)$$

where N_A is the Avogadro number, $\hbar$ is the reduced Planck constant, k is the Boltzmann constant, μ is the reduced mass, and E_r are the resonance energies in the c.m. frame;

$$(\omega\gamma)_r = \frac{(2J_r+1)}{6}\left(\frac{\Gamma_p}{\Gamma}\Gamma_\gamma\right)_r, \qquad (2)$$

are the resonance strengths, where J_r are the spins of the resonances, Γ_p and Γ_γ are the proton and γ-ray partial-decay widths, respectively, and $\Gamma = \Gamma_p + \Gamma_\gamma$ are the total widths (other decay channels are closed at the excitation energies measured in the present work). The factor of 1/6 is derived from the spins of the reactants: ^{30}P$(J^\pi = 1^+)$ and ^{1}H$(J^\pi = 1/2^+)$. The explicit exponential dependencies of the rate on the resonance energies and the linear dependencies on the proton branching ratios Γ_p/Γ and spins J_r are of particular relevance to the present work. There also exist implicit exponential dependencies of Γ_p on the corresponding resonance energies and strong dependencies of Γ_p on the corresponding J_r^π due to the Coulomb and angular-momentum barriers, respectively.

*wrede@u.washington.edu
†Present address: Pacific Northwest National Laboratory, Richland, WA 99352, USA.
‡Present address: Physics Division, Argonne National Laboratory, Argonne, IL 60439, USA.
§Present address: Physik Department E12, Technische Universität München, D-85748, Garching, Germany.

Experimental information on ^{31}S levels above the 6133.0(15) keV proton threshold [13] is incomplete, with most information up to 1998 coming from one- and two-nucleon transfer reactions on ^{32,33}S and ^{29}Si [14,15]. The lack of a radioactive ^{30}P beam of sufficient intensity ($>10^6$ s^{-1}) to make direct measurements of ^{30}P$(p,\gamma)^{31}$S resonance strengths has motivated several recent indirect studies of ^{30}P + p resonances [16–19]. Kankainen *et al.* [16] inferred resonance energies for $E_r \geqslant 788$ keV by measuring the ^{31}Cl β^+-delayed proton spectrum and assuming that proton decays of ^{31}S levels proceed to the ^{30}P ground state. Their simultaneous measurement of β^+-delayed γ rays suggested the first $T = 3/2$ level to lie at 6280(2) keV. Using the ^{12}C(^{20}Ne, $n\gamma$) reaction, Jenkins *et al.* [17,18] observed several proton unbound, high spin, γ-decaying ^{31}S levels that are not expected to be particularly relevant astrophysically. However, the authors did compile available information on ^{31}S levels with $E_r < 737$ keV to calculate an experimentally determined ^{30}P$(p,\gamma)^{31}$S reaction rate for the first time (up to 1 GK) [18]. Their reaction rate agreed well with HF calculations [12] for $T > 0.3$ GK, and deviated by up to an order of magnitude for $0.1 < T < 0.3$ GK where the effects of individual resonances are most important. Most recently, Ma *et al.* [19] used a DWBA analysis of their ^{32}S(p,d) measurement to extract spectroscopic information on proton-unbound ^{31}S levels. Although their experiment populated 17 resonances, the 80 keV-FWHM energy resolution precluded the separation of closely spaced levels. They evaluated the ^{30}P$(p,\gamma)^{31}$S reaction rate up to $T = 10$ GK for the first time by considering resonances with $E_r \leqslant 1022$ keV, with similar results to those in Ref. [18] for $T < 1$ GK because of similar experimental inputs. For $T > 1$ GK, where the HF rate is expected to be robust, their reaction rate deviated from HF estimates [12] with increasing temperature by up to an order of magnitude.

Generally, experimental information on ^{31}S above the proton threshold is still lacking despite these recent measurements. The higher level density of the ^{31}S mirror, ^{31}P, above $E_x = 6$ MeV reveals that there should be many undiscovered ^{30}P + p resonances [14]. Moreover, most of the known resonances have unknown spins and parities, unmeasured partial widths, and large uncertainties in energy. We recently reported [20] a measurement of ^{31}S levels in the energy range of interest to ONe novae ($6133 < E_x < 6700$ keV) using the nonselective ^{31}P(^{3}He, t)^{31}S reaction. The experiment excited all eight known resonances in this energy range, one tentatively known resonance, and three new resonances [two of these likely dominate the ^{30}P$(p,\gamma)^{31}$S reaction rate for $T <$ 0.25 GK]. The uncertainties in the resonance energies were also reduced significantly, which reduced the related uncertainty in the reaction rate exponentially. Incorporating our new data, the ^{30}P$(p,\gamma)^{31}$S reaction rate was found to agree with HF calculations [12] within a factor two for $0.08 < T <$ 0.40 GK. The data set discussed in Ref. [20] was a subset of data from our study of ^{31}S across a broad range of excitation energies ($4970 < E_x < 9430$ keV). In the present article we report the bulk of our ^{31}S measurements and reevaluate the resonant ^{30}P$(p,\gamma)^{31}$S reaction rate over the broad temperature range $0.01 \leqslant T \leqslant 10.00$ GK using experimental information wherever possible.

II. EXPERIMENTAL PROCEDURE

The objective of our study was to search for new ^{30}P + p resonances, and to constrain the resonance energies, spins and proton branching ratios with the ultimate goal of reevaluating the thermonuclear ^{30}P$(p,\gamma)^{31}$S reaction rate. To this end, we measured the ^{31}P(^{3}He, t)^{31}S, ^{31}P(^{3}He, t)^{31}S$^*(p)^{30}$P, and ^{32}S$(d,t)^{31}$S reactions at Yale University's Wright Nuclear Structure Laboratory where the tandem Van de Graaff provided accelerated ion beams. In each case, an Enge split-pole magnetic spectrograph was used with a position-sensitive ionization drift chamber (PIDC) [21] at the focal plane backed by a plastic scintillator to identify tritons corresponding to excited states in ^{31}S and measure their energies. The Yale Lamp Shade Array (YLSA) [22] of silicon-strip detectors was mounted at backward angles to detect coincident proton emission in the ^{31}P(^{3}He, t)^{31}S$^*(p)^{30}$P measurement.

A. ^{31}P(^{3}He, t)^{31}S singles measurement

The Yale tandem Van de Graaff was used to accelerate ^{3}He ions to 20 or 25 MeV with intensities up to 50 pnA. Ion-optical elements were used with readings of current from removable collimators and a beam dump to center the beam spot on target and tune it to <2 mm in diameter. Elemental phosphorus targets of $\approx$160 μg/cm^2 thickness were made at Duke University by evaporating red-phosphorus powder onto 20-μg/cm^2 carbon backings supported by aluminum target frames using the two-step-heating vacuum-evaporation method described in Refs. [23–25]. A 125-μg/cm^2 aluminum foil target was used for momentum calibration of the focal plane. Target thicknesses were determined to an uncertainty of 10% by measuring the energy loss of 5.486-MeV ^{241}Am α-particles through the targets with a silicon surface-barrier detector before and after beam exposure. The before/after measurements were consistent in all cases.

The spectrograph accepted reaction products through a rectangular aperture of variable solid angle, and momentum analyzed them. Tritons were focused on the PIDC, which spanned the focal plane over bending radii $70 < \rho < 87$ cm. This detector measured position via two independent, lumped delay-line readouts. A cathode measured the energy loss, ΔE, of the particles as they traversed 11 cm of 100-torr isobutane gas. The residual energy, E, of particles was measured with a backing scintillator, optically coupled to photomultipliers at each end. The cathode signal was used to produce a 10-μs gate for an ADC that processed all other electronics channels. Using the cathode as the trigger minimized the event rate in comparison to using the scintillator, which is susceptible to background from neutrons and light leaks.

Triton singles measurements of the ^{31}P(^{3}He, t)^{31}S reaction were made at $E(^3\text{He}) = 25$ MeV, $B = 11$ kG, and $\theta_{\text{lab}} = 1^\circ$ and 10° with nominal horizontal and vertical aperture settings of $\Delta\theta = \pm 10$ mrad and $\Delta\phi = \pm 40$ mrad, respectively. To improve triton dispersion at the focal plane, singles measurements were made at $E(^3\text{He}) = 20$ MeV with the spectrograph set to $B = 9$ kG at $\theta_{\text{lab}} = 1^\circ$, 10°, and 20°. A relatively high-statistics spectrum was acquired at $\theta_{\text{lab}} = 1^\circ \pm 10$ mrad using a beam energy of 20 MeV with the magnetic field reduced to 8.5 kG. This spectrum was acquired while testing YLSA for

the t-p coincidence measurement (described in Sec. III B), which contributed an additional high-statistics triton spectrum with the settings $\theta_{\rm lab} = 1.5^\circ \pm 20$ mrad, $B = 8.5$ kG, and $E(^3\mathrm{He}) = 20$ MeV. For each set of experimental parameters, a corresponding ^{27}Al(^{3}He, t)^{27}Si spectrum was acquired during the same experimental run for energy calibration. The 20-MeV data set was discussed in our previous report [20] over the limited excitation-energy range relevant to novae.

B. ^{31}P(^{3}He, t)^{31}S*(p)^{30}P coincidence measurement

The ^{31}P(^{3}He, t)^{31}S*(p)^{30}P coincidence measurement was made by coupling the magnetic-analysis apparatus to the Yale Lamp Shade Array in order to detect protons at backward angles in coincidence with tritons at the PIDC. YLSA is an array of five 1/8 circular-sector silicon-strip detectors with 16 annular strips apiece [26]. The sectors cover an angular range $130^\circ \lesssim \theta_{\rm lab} \lesssim 165^\circ (\approx 14\%$ of the laboratory solid angle), and are arranged in a pentagonal pyramid or "lamp shade" configuration (Fig. 1) such that the beam travels through an aperture at the vertex as shown in Fig. 2. Due to a damaged detector sector, the experiment employed four active sectors. Ideally, the spectrometer would have been positioned at 0° for the coincidence measurement since this would have aligned the proton-decay axis of symmetry with the beamline/YLSA axis, and simplified the analysis by minimizing both the population of $m \neq 0$ magnetic substates in ^{31}S and the angular overlap of YLSA bins [22]. However, a prohibitively high event rate was observed in the PIDC at this angle due to the scattering of beam ions entering the spectrometer. For the experiment, the spectrometer was moved to $\theta_{\rm lab} = 1.5^\circ$ where most of the scattered beam was eliminated. This angle was sufficiently small to ensure a negligible population of $m \neq 0$ magnetic substates ($\lesssim$1% compared with $\gtrsim$5% statistical uncertainties) and smearing of angular bins (verified using Monte Carlo simulations [22]). A beam energy of 20 MeV and aperture settings of $\Delta\theta = \pm 20$ mrad and $\Delta\phi = \pm 40$ mrad were chosen as a compromise between energy resolution and statistics, and a magnetic-field setting of $B = 8.5$ kG centered tritons corresponding to the excitation energies of interest in ^{31}S on the detector.

The silicon detectors were moderately radiation damaged from prior use. To minimize an observed [27] rise in leakage current from beam-induced δ electrons charging the exposed oxide between strips on the front side of the detectors, they were flipped so that protons entered through the uniform back side. In addition, cobalt magnets were attached to the target ladder to suppress ejected electrons, and +600 V was applied to the target ladder and YLSA mount to attract electrons away from the detector surfaces. The 500-μm thick detectors were over depleted using a reverse bias of 95 V.

To optimize timing resolution in the ^{31}P(^{3}He, t)^{31}S*(p)^{30}P coincidence experiment, the fast scintillator signal from the anode of the photomultiplier tube was used to set the gate for all ADCs and as the start signal for all TDCs. The ECL signals output by the YLSA amplifiers were delayed by 250 ns

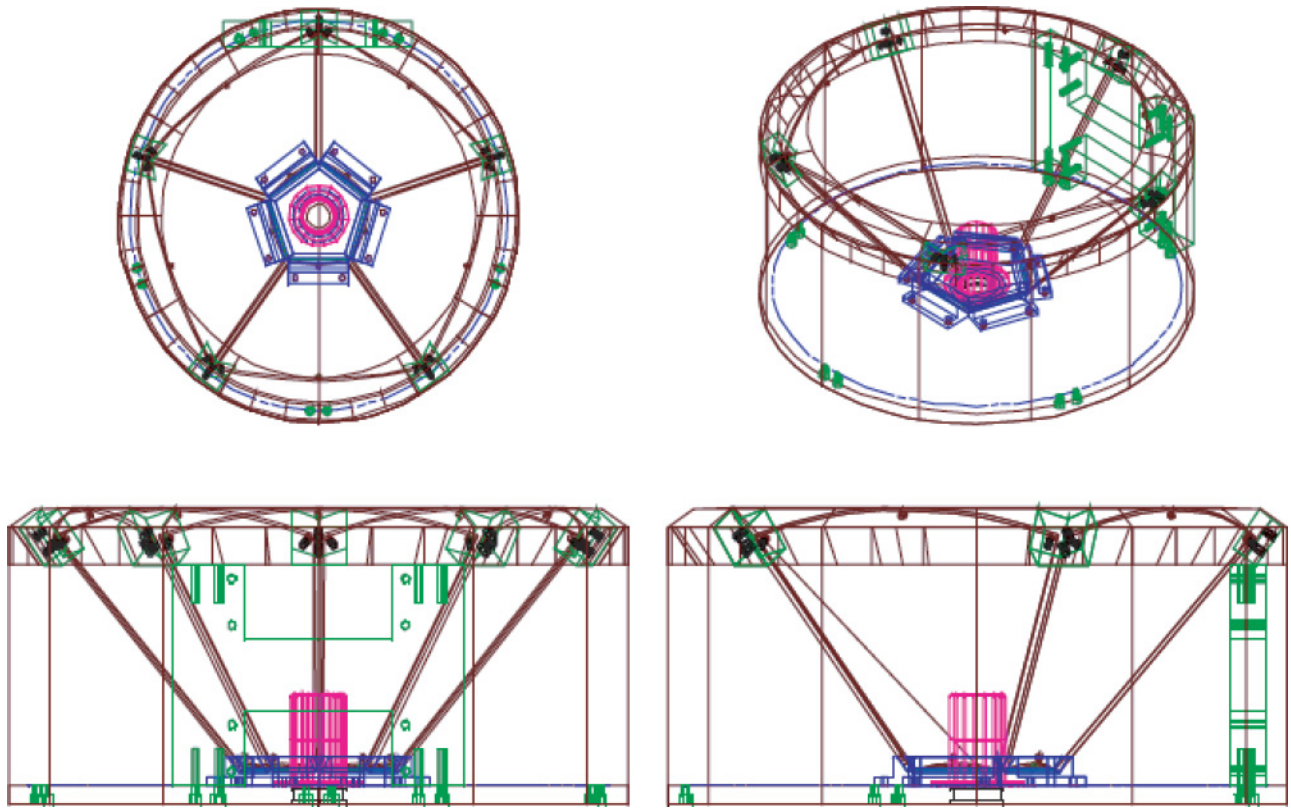

FIG. 1. (Color online) Three-dimensional computer-aided design drawings of YLSA's five silicon strip detectors fastened to the YLSA mount (to scale).

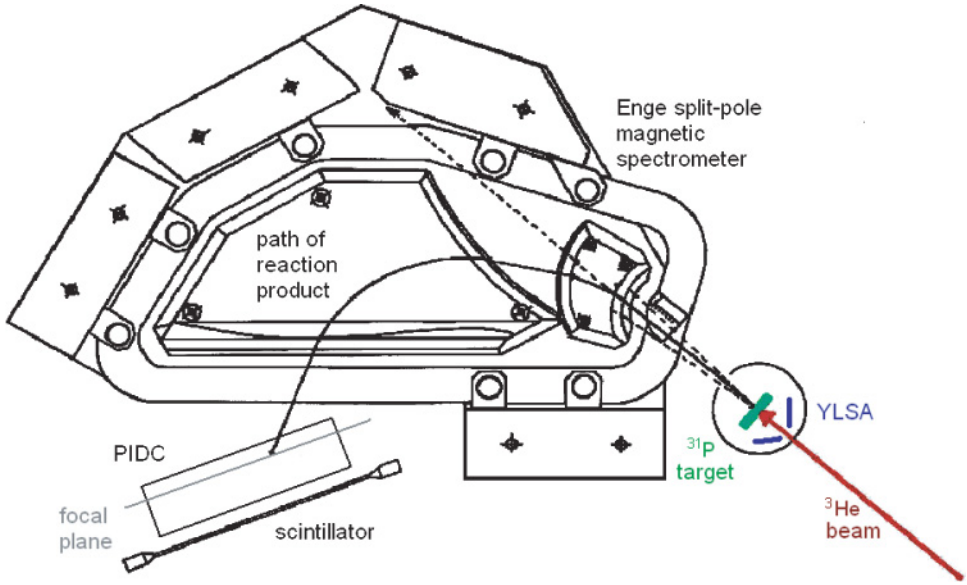

FIG. 2. (Color online) Schematic of experimental apparatus including a drawing of the Enge split-pole magnetic spectrometer (to scale) set to zero degrees with a schematic representation of the beam (red online), target (green online), scattering chamber, YLSA (blue online), and focal-plane detector including the PIDC (focal plane in gray) and scintillator (not to scale).

and used as the TDC stop signals. In the absence of a cathode-scintillator coincidence, the scintillator gate was fast cleared in the ADCs and TDCs to minimize the dead time. Scalers of total events presented to—and events accepted by—the acquisition were used to monitor the dead time ($\lesssim$5%).

For all measurements, data were transferred from the VME crate that housed the digitizers to a personal computer running the Vx-works operating system where it was stored in an 8-kbyte memory buffer. When the buffer filled, events were transferred via private Ethernet to a workstation where they could be viewed online using the Java-based data acquisition and display package JAM [28], and stored for offline sorting and analysis.

C. ^{32}S$(d,t)^{31}$S singles measurement

Measurements of the ^{32}S$(d,t)^{31}$S reaction were made using the same apparatus as the $(^3\mathrm{He},t)$ singles measurements. A 25-MeV deuteron beam of up to 40 pnA intensity, a 150 μg/cm^2 CdS target evaporated on a 20 μg/cm^2, natural carbon substrate, and magnetic field strengths of $B = 9.5$ or 10.5 kG were used. The horizontal and vertical apertures were set to $\Delta\theta = \pm 10$ or 20 mrad and $\Delta\phi = \pm 20$ or 40 mrad, and spectra were acquired at $\theta_{\mathrm{lab}} = 7.5^\circ, 10^\circ, 15^\circ, 20^\circ, 25^\circ, 30^\circ$, and 40° over a total period of one week. To calibrate the focal plane, (d,t) spectra were also acquired at each angle using a SiO target during the same week.

III. DATA AND ANALYSIS

A. ^{31}P$(^3\mathrm{He},t)^{31}$S singles measurement

Particle groups (p,d,t,α) were identified using the focal-plane detector by combining focal-plane position, cathode (ΔE), and scintillator (E) signals in two-dimensional histograms. Tritons were selected cleanly by sorting the data offline through software gates in these histograms using JAM, and spectra of focal-plane position were plotted for the ^{31}P$(^3\mathrm{He},t)^{31}$S (Fig. 3) and ^{27}Al$(^3\mathrm{He},t)^{27}$Si reactions. Additional selection was provided by imposing a coincidence requirement on position signals from the two delay lines of the PIDC.

The triton spectra exhibited no evidence for background peaks from $(^3\mathrm{He},t)$ reactions on target contaminants. Tritons from the ^{12}C$(^3\mathrm{He},t)$ and ^{16}O$(^3\mathrm{He},t)$ reactions were kinematically excluded at the detector position. The ^{13}C$(^3\mathrm{He},t)$ reaction produced a diffuse, low-intensity background that was measured to be negligible with an isotopically enriched ^{13}C target. Data acquired with a melamine ($C_3H_6N_6$) target showed that nitrogen presented no significant background. Kinematic analysis was used to exclude other potential spectral contaminants.

The spectra were analyzed using a least-squares fit of multiple $\approx$25 keV-FWHM Gaussian and exponentially modified Gaussian (asymmetric to account for a low energy triton tail) functions; from these fits peak centroids were extracted. Self-consistent analyses using each of the two independent fits produced consistent excitation energies for isolated peaks, but the exponentially modified Gaussian fits were more effective for fitting multiplets because of the more realistic line shape. There was no strong evidence for resonances with decay widths Γ similar to (or greater than) the instrumental resolution so peak widths were held fixed to the instrumental width, which was measured separately for each spectrum by fitting isolated peaks corresponding to bound states. Identification and isolation of ^{31}S levels above $E_x = 6.7$ keV was aided by a comparison of singles and coincidence spectra (Sec. III B).

The forward-angle differential cross sections of the ^{31}P$(^3\mathrm{He},t)^{31}$S reaction to individual ^{31}S excited states observed at 20-MeV ^{3}He-beam energy were estimated to be in the range $0.05 \lesssim d\sigma/d\Omega \lesssim 10$ μb/sr. The average differential cross-section was larger by a factor $\approx$4 for the $E(^3\mathrm{He}) =$ 25-MeV runs. Cross sections for the ^{27}Al$(^3\mathrm{He},t)^{27}$Si reaction were similar.

Isolated, easily identifiable excited states of ^{27}Si in the energy range $5 < E_x < 9$ MeV [from the ^{27}Al$(^3\mathrm{He},t)^{27}$Si reaction] with uncertainties as low as 0.4 keV (but typically 3 keV) were used for an initial calibration of the focal

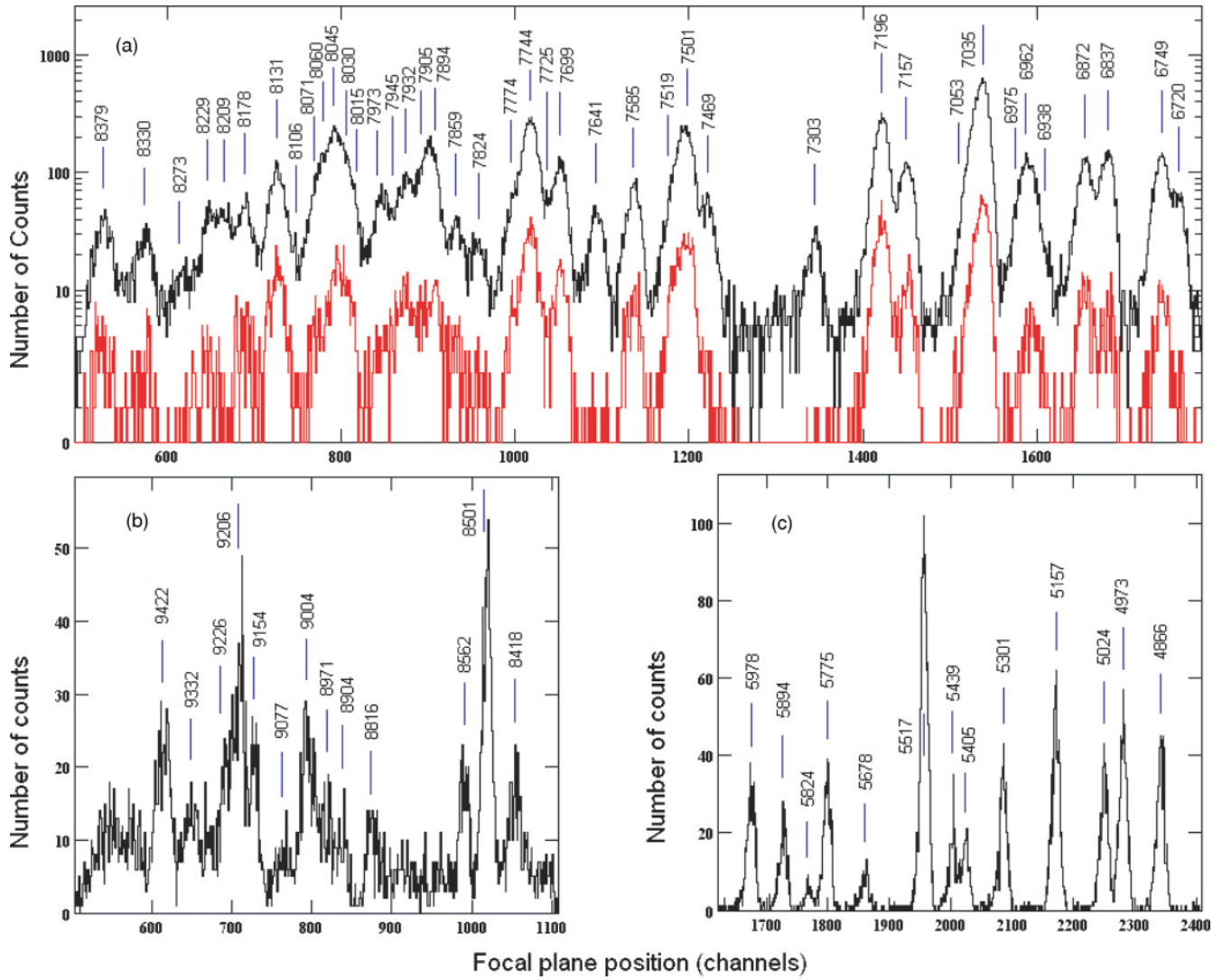

FIG. 3. (Color online) Portions of selected ^{31}P(^{3}He, t)^{31}S focal-plane spectra with observed peaks labeled by adopted E_x (keV) derived from averaging values from the present work with those from previous work (Table I). Panel (a) shows both triton-singles events (black) and candidate-coincidence events (gray; red online); panels (b) and (c) show only triton-singles events. Experimental parameters: (a) $E(^3\text{He}) = 20$ MeV, $\theta_{\text{lab}} = 1.5^\circ$, $\Delta\theta = \pm 20$ mrad; (b) $E(^3\text{He}) = 25$ MeV, $\theta_{\text{lab}} = 1.0^\circ$, $\Delta\theta = \pm 20$ mrad; (c) $E(^3\text{He}) = 20$ MeV, $\theta_{\text{lab}} = 10.0^\circ$, $\Delta\theta = \pm 10$ mrad. For $6.0 < E_x < 6.7$ MeV see Ref. [20].

plane for each data set. Second-degree polynomial least-squares fits of bending radius ρ to focal-plane position (with $0.94 \leqslant \chi^2_\nu \leqslant 1.32$[1]) were derived from known ^{27}Si excitation energies [14] and measured peak centroids. These fits were used to identify ^{31}S levels and determine their excitation energies to an uncertainty of 3 keV. This uncertainty included contributions from statistical uncertainties in the peak centroids (typically $\leqslant 1$ keV), uncertainty in the relative Q values of the ^{27}Al(^{3}He, t)^{27}Si and ^{31}P(^{3}He, t)^{31}S reactions (1.5 keV) [13,32], uncertainty in relative ^{27}Al-to-^{31}P target thicknesses (2 keV), and reproducibility ($\approx$1 keV). Under the assumptions that these uncertainties were Gaussian distributed and mutually independent, they were added in quadrature.

Precisely known ^{31}S levels[2] at 5978.2(7) keV, 6160.2(7) keV, 6636.3(15) keV, and 7302.8(8) keV [18] were clearly identified and used for an internal calibration of the ^{31}S spectra with $0.56 \leqslant \chi^2_\nu \leqslant 1.99$ (fits for the two high statistics spectra, which carry the most weight, had $\chi^2_\nu = 0.56$ & 0.73). This eliminated systematic uncertainties associated with using a different target for the calibration and yielded a 2-keV excitation-energy uncertainty in the important energy

[1]The χ^2_ν values quoted in this paragraph exclude the 25-MeV data, which were of relatively poor quality due to low statistics and poor energy resolution. The calibrations for the 25-MeV measurements yielded $1 \lesssim \chi^2_\nu \lesssim 2$, but these measurements only played a significant role in the weighted averages of excitation energies above 8.4 MeV where unpublished data were used for calibration [29–31].

[2]Where excitation-energy uncertainties are not quoted directly in Refs. [17,18], they are derived from the γ-ray energy uncertainties in Refs. [17,18].

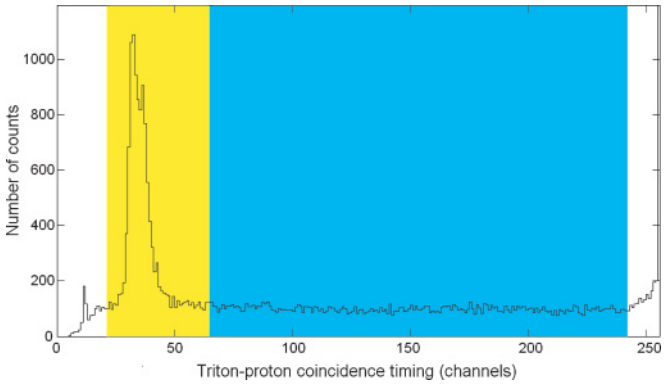

FIG. 4. (Color online) Triton-proton timing spectrum for the ^{31}P(^{3}He, t)^{31}S*(p)^{30}P reaction. Experimental settings: $E(^3\text{He}) = 20$ MeV, $\theta_{\text{lab}} = 1.5^\circ$, $\Delta\theta = \pm 20$ mrad, and $B = 8.5$ kG. Events in the (lighter gray; yellow online) shaded region were considered to be candidate t-p coincidence events. Events in the (darker gray; blue online) shaded region were used to determine the rate of accidental coincidences for each resonance. The scale of the abscissa is ≈5 ns per channel.

range $6000 \lesssim E_x \lesssim 7300$ keV. The results were consistent with those from the ^{27}Si calibration. For levels outside the internal-calibration energy range in the high-statistics spectra, the internal ^{31}S calibration points were used together with the ^{27}Si calibration points to provide a final calibration for each of those data sets ($\chi^2_\nu = 0.65$ & 0.92).

B. ^{31}P(^{3}He, t)^{31}S*(p)^{30}P coincidence measurement

As discussed in Sec. II B the measurement of the ^{31}P(^{3}He, t)^{31}S*(p)^{30}P reaction was made using the silicon-detector array YLSA. YLSA strips were gain matched using known α-particle decay lines of energy $5 < E_\alpha < 9$ MeV from a ^{228}Th source. The effective energy threshold for detection of protons was found to be between 500 and 600 keV using the strong ^{31}P(^{3}He, α)^{30}P*(p)^{29}Si$_{\text{g.s.}}$ reaction and the detailed level scheme of ^{30}P. Because the energy threshold was not constant from strip to strip, the branching ratios for the lowest-energy $^{30}\text{P} + p$ resonances likely suffered from deficiencies that were difficult to estimate. An in-situ timing calibration was obtained using $\alpha - p$ coincidences from the ^{31}P(^{3}He, α)^{30}P*(p)^{29}Si$_{\text{g.s.}}$ reaction and was cross checked with an offline calibration using a pulser signal that was split and input to the YLSA pre-amplifier motherboards and scintillator electronics.

Candidate proton decays to the $J^\pi = 1^+$ ground state of ^{30}P(p_0 decays) were selected offline by sorting the data through software gates using JAM. A conservative 200-ns gate was imposed on the YLSA vs. scintillator t-p timing peak (≈40 ns-FWHM), as shown in Fig. 4. A gate was imposed on the diagonal band corresponding to p_0 decays in the YLSA energy vs. focal-plane position two-dimensional histogram (Fig. 5) that was cleanly resolved from decays to the first two ^{30}P excited states at $E_x(^{30}\text{P}) = 677$ and 709 keV ($p_{1,2}$ decays, respectively). One and only one strip in YLSA was required to register a hit in coincidence with each triton gate (multiplicity =1). Triton spectra of candidate t-p coincidence events were plotted for four proton angular ranges, and for the sum of all angles (Fig. 3). Each spectrum was fit with a template of exponentially modified Gaussian functions with the widths and positions fixed to the same values used in the singles-spectrum fit, and the amplitudes free to vary. The rate of random coincidences was estimated for each peak by an identical analysis with a 900-ns gate set on the constant background in the timing spectrum. Using this rate, a subtraction was made to account for random coincidences. Monte Carlo kinematics simulations were used to determine the geometrical efficiency and angular centroid of each YLSA angular bin in the c.m. frame to a fraction of a percent for each resonance [22].

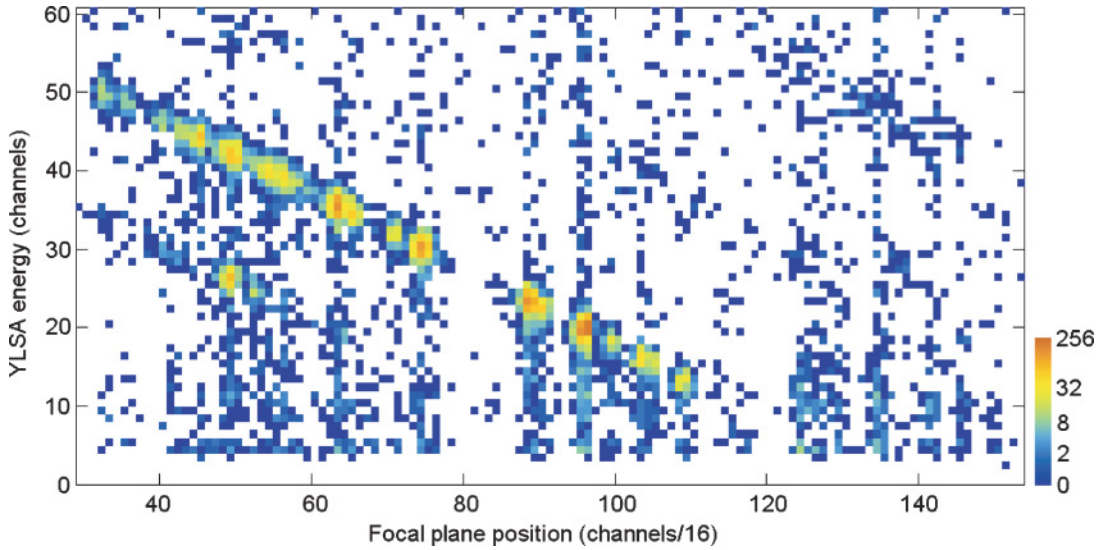

FIG. 5. (Color online) 2-D spectrum of candidate t-p coincidence events from the ^{31}P(^{3}He, t)^{31}S*(p)^{30}P reaction. The graded logarithmic scale indicates the number of counts per bin. The most prominent diagonal band corresponds to proton decays of resonances in ^{31}S to the ground state of ^{30}P (p_0 decays). The parallel band ≈15 channels below corresponds to mutually unresolved decays to one or both of the first two excited states of ^{30}P ($p_{1,2}$ decays). The data set presented is the same as that in panel (a) of Fig. 3.

Dividing the background-subtracted amplitudes of the coincidence-spectrum peaks (corrected for the geometrical efficiency of YLSA) by the amplitudes of the corresponding singles-spectrum peaks yielded t-p angular correlations that were plotted in 4 angular bins; this choice of binning optimized the compromise between statistics per angular bin and angular resolution. Each point in the angular correlation was corrected upward by 11(1)% to account for good events with multiplicity >1 that result when a proton in one strip is coincident with background or noise counts in other strips. This global correction was estimated by analyzing events with multiplicities two [10(1)%] and three [1.0(2)%].

Under the assumptions that the nuclear levels being considered are isolated and have definite parity, each angular correlation is described by a linear combination of even Legendre polynomials $P_n(\cos\theta_{\mathrm{c.m.}})$,

$$W(\theta_{\mathrm{c.m}}) = \frac{1}{4\pi}[a_0 + a_2 P_2(\cos\theta_{\mathrm{c.m.}}) + a_4 P_4(\cos\theta_{\mathrm{c.m.}}) + \cdots], \tag{3}$$

that are symmetric about $\theta_{\mathrm{c.m.}} = 90^\circ$ [22,33,34]. The sum is truncated at a maximum value of $n = 2\ell$, where ℓ is the proton orbital angular momentum. For example, an $\ell = 0$ angular correlation is described by the first term of Eq. (3) at most, an $\ell = 1$ angular correlation is described by the first two terms at most, and so on. Beginning with an isotropic ($n = 0$) fit of Eq. (3) to the angular-correlation data for a particular ^{31}S level of unknown J^π, terms of successively higher n may be added to Eq. (3) until a sufficiently good fit is obtained. The minimum number of terms needed to fit each t-p angular correlation may be used to determine a minimum value of ℓ, ℓ_{min}, that can in turn be used to constrain J^π of the corresponding ^{31}S level. In the present experiment, the poor statistics and limited angular range of the measurements made it impossible to rule out the possibility of terms with $\ell > \ell_{\mathrm{min}}$ completely. Equation (3) is normalized such that extrapolating and integrating $W(\theta_{\mathrm{c.m.}})$ over 4π sr for each level yields the proton-branching ratio of that level to the ground state of ^{30}P.

The t-p coincidence peaks corresponding to 17 levels were sufficiently isolated and populated to be individually tested for anisotropic angular correlations (Fig. 6); this was accomplished using χ^2_ν p-value hypothesis testing. The first step in such an analysis is the statement of a null hypothesis: we chose the isotropic fit ($n = 0$) as the initial null hypothesis for each level and extracted a χ^2_ν value for this fit. The p value is the probability that a value chosen at random from the χ^2_ν probability distribution would be greater than or equal to the observed value if the null hypothesis were true. If the χ^2_ν p value was >0.05 for the isotropic fit (the null hypothesis), then the null hypothesis was accepted and the angular correlation was assigned a minimum proton orbital angular momentum of $\ell_{\mathrm{min}} = 0$. If the χ^2_ν p value was <0.05 for the isotropic fit, then the null hypothesis was rejected and the second ($n = 2$) term of Eq. (3) was added to the fit, forming a new null hypothesis that was tested by the same method. Terms were added one-by-one until the χ^2_ν p value was >0.05 for a null-hypothesis fit (at that point the fit was deemed sufficient) to a maximum of three terms. This maximum number of terms was dictated by the fact that a χ^2_ν analysis cannot be performed on four data points using a fit function with four free parameters or more. Anisotropic angular-correlation fits were constrained to be physical: $W(\theta_{\mathrm{c.m.}}) \geqslant 0$ at all angles and $\Gamma_p/\Gamma \leqslant 1$.

The fit corresponding to the accepted ℓ_{min} value of each angular correlation was integrated over 4π sr to determine the proton-branching ratio of the corresponding ^{31}S level. The branching-ratio uncertainties incorporated the possibility of higher-n terms. For example, when $\ell_{\mathrm{min}} = 0$, there is often a significant probability that $\ell = 1$. An $n \leqslant 2$ fit generally yields a branching ratio much less than an $n = 0$ fit to the same data because of the usual minimum in the angular correlation at $\theta_{\mathrm{c.m.}} = 90^\circ$. Similarly, an $n \leqslant 4$ fit can yield a branching ratio greater than an $n \leqslant 2$ fit to the same data because of the possible enhancement at $\theta_{\mathrm{c.m.}} = 90^\circ$. Upper and lower uncertainty bounds were estimated by finding the maximum and minimum branching ratios, respectively, for $\ell_{\mathrm{min}} \leqslant \ell \leqslant 2$, and adding linearly the 1σ statistical error from the $n = 0$ fit at both limits. The probability-density function is unique and non-trivial in each case due to the uncertainty in ℓ. This complicates the statistical interpretation of these uncertainties and, therefore, we do not assign a confidence level to these error bars. When statistics were too low to plot a meaningful angular correlation, an isotropic angular correlation was assumed to determine the branching ratio, Γ_p/Γ, and the possibility of $n > 0$ terms was incorporated into the uncertainty by placing the upper and lower bounds of the branching-ratio uncertainty at $\Gamma_p/\Gamma + 1\sigma$ and $0.5\Gamma_p/\Gamma - 1\sigma$, respectively. These bounds were estimated by examining higher-statistics cases. In cases where $\Gamma_p/\Gamma - 2\sigma < 0$, a 90% C.L. upper limit, UL, was estimated by constraining the probability density function [assumed in these cases to be a Gaussian, $g(\Gamma_p/\Gamma)$] to positive values and numerically solving $\int_0^{UL} g(\Gamma_p/\Gamma)\,d(\Gamma_p/\Gamma) / \int_0^{\infty} g(\Gamma_p/\Gamma)\,d(\Gamma_p/\Gamma) = 0.90$. In one case where Γ_p/Γ was consistent with both 0 and 1, nothing could be said.

Under the assumption that p_0 decays proceed via the lowest-allowed ℓ transfer [and using $J^\pi(^{30}\mathrm{P}) = 1^+$ and $J^\pi(p) = 1/2^+$] the J^π values for $^{30}\mathrm{P} + p$ resonances with a given value of ℓ are [$\ell = 0$, $J^\pi = (1/2, 3/2)^+$]; [$\ell = 1$, $J^\pi = (1/2, 3/2, 5/2)^-$]; [$\ell = 2$, $J^\pi = (5/2, 7/2)^+$]; [$\ell = 3$, $J^\pi = (7/2, 9/2)^-$]; and so on. To set tentative upper limits on J^π we assumed that levels with finite proton branches measured in the present work, and excitation energies less than 7.0 MeV, decay by angular-momentum transfer $\ell \leqslant 3$. This assumption was based on our estimate using Eq. (4) that $\ell > 3$ proton decays will have $\Gamma_p \lesssim 10$ meV at these low proton energies and in most cases will not be competitive with γ decay. We use the following notation to report the tentative $J^\pi(^{31}\mathrm{S})$ constraints (for levels with $E_x < 7.0$ MeV) corresponding to each value of ℓ_{min} as follows: [$\ell_{\mathrm{min}} = 0$, $J^\pi = (1/2^+ - 9/2^-)$]; [$\ell_{\mathrm{min}} = 1$, $J^\pi = (1/2^- - 9/2^-)$]; [$\ell_{\mathrm{min}} = 2$, $J^\pi = (5/2^+ - 9/2^-)$]; [$\ell_{\mathrm{min}} = 3$, $J^\pi = (7/2^-, 9/2^-)$]. For example, an $\ell_{\mathrm{min}} = 1$ determination would tentatively constrain $J^\pi = (1/2^-, 3/2^-, 5/2^-, 5/2^+, 7/2^+, 7/2^-, 9/2^-) \equiv (1/2^- - 9/2^-)$. Similarly, we assumed that proton-decaying levels with $7.0 < E_x < 7.5$ MeV decay by angular-momentum transfer $\ell \leqslant 4$, and those with $7.5 < E_x < 8.4$ MeV decay by angular-momentum transfer $\ell \leqslant 5$. If ℓ_{min} was determined by a p value $\leqslant 0.0001$ for the $n = 2(\ell_{\mathrm{min}} - 1)$

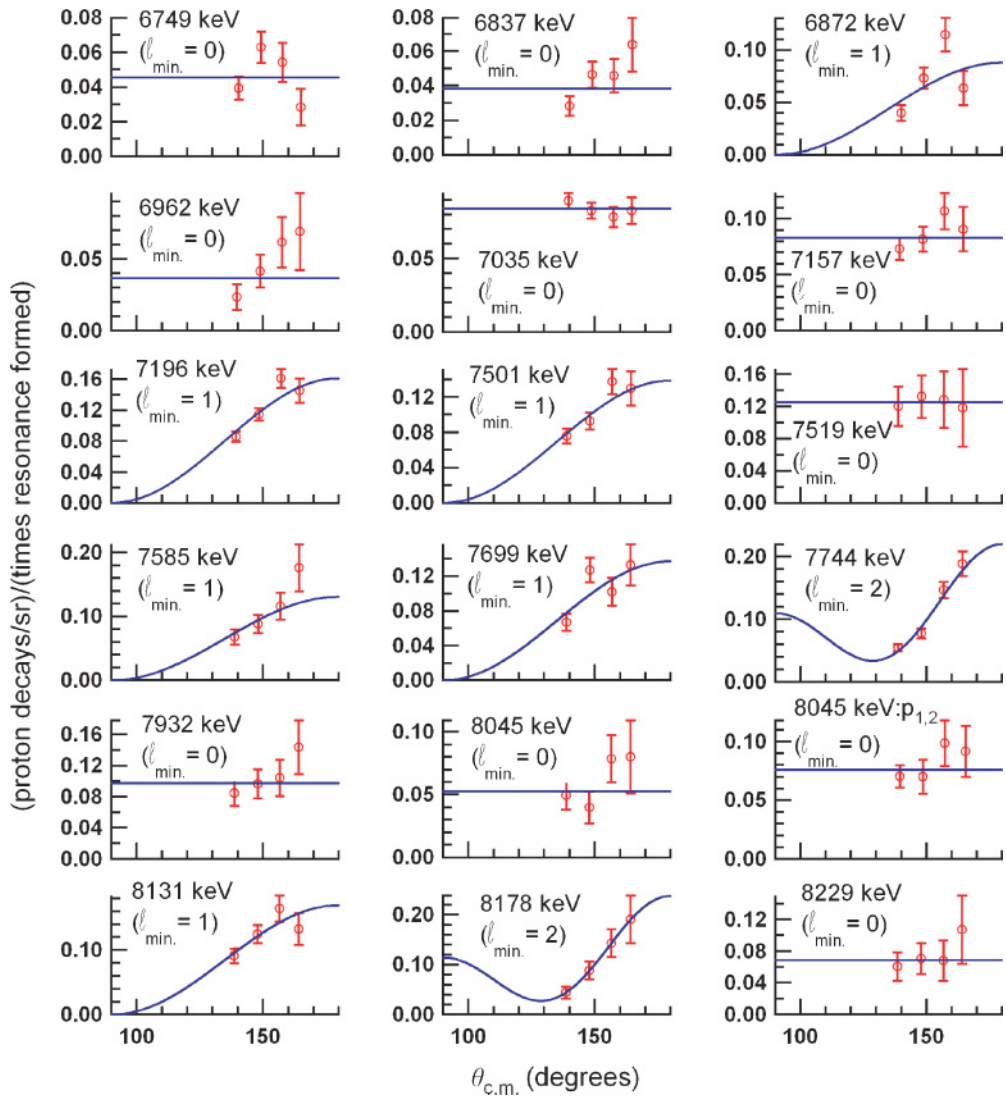

FIG. 6. (Color online) Triton-proton angular correlations from the ^{31}P(^{3}He, t)^{31}S*(p)^{30}P reaction at 20 MeV. Each angular correlation is labeled by its adopted excitation energy from Table I, and the minimum proton orbital angular momentum, $\ell_{\min}$, deduced from the minimum number of even Legendre-polynomial terms required to provide a sufficient fit as outlined in the text. The label $p_{1,2}$ denotes the sum of the angular correlations from decays to the first two excited states in ^{30}P. For the 6749 keV level, the isotropic distribution shown was used to determine the branching ratio because the $n = 0$, $n \leqslant 2$, and $n \leqslant 4$ fits were all poor.

fit, we report a firmer, unbracketed lower limit on J^{π} that is, nevertheless, dependent on the assumption that the proton decay proceeds via the lowest-allowed ℓ transfer. Although we expect this assumption to hold in most cases, there are known cases where it does not [34].

For some levels we observed decays to one or both of the first two excited states in ^{30}P at 677 and 709 keV [$(J^{\pi}, T) = (0^{+}, 1)$ and $(1^{+}, 0)$, respectively]; these are separated by only 32 keV and were not mutually resolved in YLSA. Identical analysis techniques were used to determine the summed proton-branching ratio to these two levels, $\Gamma_{p_{1,2}}/\Gamma \equiv (\Gamma_{p_1} + \Gamma_{p_2})/\Gamma$.

In general, because of the large uncertainties emerging from the low coincidence statistics and the extrapolation of the limited angular range of the proton-decay measurements, additional systematic uncertainties do not contribute significantly to the branching-ratio uncertainties in the present work. The branching ratios and spin-parity constraints are discussed in depth in the Appendix, and are summarized in Table I.

C. ^{32}S(d, t)^{31}S singles measurement

The (d, t) analysis was done in a similar fashion to the $(^{3}\mathrm{He}, t)$ analysis. The spectrum in Fig. 7 shows the region of astrophysical interest. Peaks were fit with ≈25 keV-FWHM Gaussian functions. In this case, peaks from the ^{12}C$(d, t)^{11}$C, ^{16}O$(d, t)^{15}$O, and ^{28}Si$(d, t)^{27}$Si reactions were used to calibrate the focal plane at each angle using spectra from the CdS- and SiO-target runs. 2nd-degree polynomial least-squares fits of bending radius ρ to focal-plane

TABLE I. Nuclear energy levels of ^{31}S. The column labeled "Endt" lists experimentally measured ^{31}S excitation energies (keV) circa 1998 [14,15]. The next six columns list more recent measurements including the present work and a weighted average under, "adopted". The J^π, T assignments incorporate all experimental work on ^{31}S including constraints from the present work. The final two columns tabulate the proton-branching ratios measured in the present work.

Endt [14,15]	(^{3}He, α) [35]	($\beta^+\nu_e$) [16]	(^{20}Ne, $n\gamma$) [17,18]	(p, d) [19]	(^{3}He, t) present	E_x adopted	J^π; T adopted	Γ_{p_0}/Γ	$\Gamma_{p_{1,2}}/\Gamma$
4969(7)	4975(5)			4988(8)	4971(3)	4973.1(23)	$3/2^-$		
5022(12)	5028(5)				5022(3)	5023.5(25)	$(1/2, 5/2^+)$[a]		
5151(6)	5161(5)			5155(5)	5158(3)	5157.1(21)	$1/2^+$		
5306(9)	5305(5)		5300.5(3)	5331(5)	5301(3)	5300.6(3)	$9/2^+$		
5408(9)					5405(3)	5405.3(28)	$(3/2-7/2)$[a]		
5440(11)					5439(3)	5439.1(29)	$(3/2-7/2)$[a]		
5515(11)	5519(5)			5497(10)	5518(3)	5516.8(24)	$(3/2-7/2)$[a]		
5685(8)	5677(5)				5678(3)	5678.4(24)	$(5/2-9/2)$[a]		
5781(8)	5775(5)	5772(2)		5781(5)	5779(3)	5775.1(15)	$5/2^+$		
5826(10)					5824(3)	5824.2(29)	$(5/2-9/2)$[a]		
5894(9)	5889(5)			5959(10)[b]	5896(3)	5894.1(25)	$(3/2, 5/2)^+$		
5985(10)	5975(5)		5978.2(7)[c]	5959(10)[b]	5981(3)[d]	5978.2(9)	$9/2^+$		
					6134(2)	6134.0(20)	$(3/2^+-9/2^+)$[a]		
6155(10)			6160.2(7)[c]		6160(3)[d]	6160.2(7)	$5/2^-$		
6267(10)	6257(5)			6267(5)	6259(2)	6259.9(17)	$1/2^+; 1/2$		
6268(10)		6280(2)			6283(2)	6281.2(14)	$3/2^+; 3/2$		
					6327(2)	6327.0(20)	$(3/2^-, 7/2^+)$[a]		
6350(11)					6357(2)	6356.8(20)	$(5/2^+)$		
			6376.9(5)		[e]	6376.9(5)	$9/2^-$		
			6393.7(5)		[e]	6393.3(5)	$11/2^+$		
6396(10)	6393(5)			6411(9)	6400(3)[f]	6399.4(22)	$(3/2^-, 5/2^-, 7/2^+)$[a]		
6543(11)				6546(15)	6543(2)	6543.1(20)	$(3/2, 5/2)^-$[a]		
[6593(15)]					6585(2)	6585.1(20)	$(3/2, 5/2, 7/2)^-$[a]		
6628(13)			6636.3(15)[c]		6639(3)[d]	6636.8(13)	$9/2^-$		
6712(11)					6720(2)	6719.8(20)	$(1/2^+-9/2^-)$	$0.25^{+0.07}_{-0.20}$[g]	
6748(10)					6749(2)	6749.0(20)	$(7/2^-, 9/2^-)$[h]	$0.57^{+0.07}_{-0.32}$[h]	
6796(25)					[i]	6796(25)			
			6833.4(3)		[6836(2)]	6833.4(3)	$11/2^-$		
6835(9)				6848(9)	6836(2)[j]	6836.5(18)	$(1/2^+-9/2^-)$	$0.48^{+0.07}_{-0.34}$[k]	
6870(10)					6872(2)	6872.0(20)	$\geqslant 1/2^-$	$0.37^{+0.09}_{-0.13}$	
6921(25)		6921(15)			6939(3)	6938.1(29)	$(1/2^+, 3/2^+, 5/2^+)$	$1.25^{+0.40}_{-1.03}$	
6990(19)[l]	6966(5)				6961(3)	6962.3(26)	$1/2^+$	$0.46^{+0.11}_{-0.40}$	
					[6975(3)]	[6975(3)]	; (3/2)	<0.38	
7006(25)[l]		7012(16)			7036(2)	7035.4(20)	$(1/2^+)$; (3/2)	$1.05^{+0.05}_{-0.05}$	
7039(10)	7033(5)			7044(6)	[7036(2)]	7038(4)	$5/2^+$		
					[7053(2)]	[7053.0(20)]	; (3/2)	$0.36^{+0.15}_{-0.33}$	
7112(25)					[i]	7112(25)			
7165(9)[m]	7156(5)	7151(6)		7144(16)	7157(2)	7156.5(17)	$(3/2, 5/2)^+$	$1.04^{+0.11}_{-0.63}$	
7199(13)					7196(2)	7196.1(20)	$\geqslant 1/2^-$	$0.67^{+0.08}_{-0.12}$	
7311(11)			7302.8(7)[c]		7301(3)[d]	7302.7(7)	$11/2^+$	<0.13	
		7347(14)			[i]	7347(14)	$(1/2^+, 3/2^+, 5/2^+)$		
7445(25)					7469(3)	7469(3)	$(1/2^+-11/2^+)$	$0.46^{+0.10}_{-0.33}$	<0.03
					7501(3)	7501(3)	$(1/2^+-13/2^-)$	$0.58^{+0.44}_{-0.09}$	<0.02
7522(20)				7510(6)[b]	7519(3)	7519(3)	$(1/2^+-13/2^-)$	$1.57^{+0.25}_{-0.97}$	<0.08
7600(30)					7585(3)	7585(3)	$(1/2^--13/2^-)$	$0.55^{+0.70}_{-0.13}$	<0.05
7660(30)			7640.3[n]		7641(3)	7641(3)	$(5/2^-, 7/2-11/2, 13/2^-)$	$0.16^{+0.05}_{-0.13}$	<0.06
		7707(8)			7698(3)	7699.1(28)	$(5/2^+)$	$0.57^{+0.11}_{-0.13}$	<0.02
7730(12)[m]	7725(5)			7728(4)	7723(3)	7725.0(21)	$1/2^-$	<0.47	$0.48^{+0.10}_{-0.34}$
					7744(3)	7744(3)	$\geqslant 5/2^+$	$1.00^{+0.06}_{-0.06}$	<0.03
[7768(25)]					7774(3)	7774(3)	$(1/2^+-13/2^-)$	$0.92^{+0.18}_{-0.64}$	<0.08
					7824(3)	7824(3)	$(1/2^+-13/2^-)$	$1.20^{+0.24}_{-0.84}$	<0.11
7850(25)					7859(3)	7859(3)	$(1/2^+-13/2^-)$	$1.25^{+0.19}_{-0.81}$	<0.07

TABLE I. *(Continued.)*

Endt [14,15]	(^{3}He, α) [35]	($\beta^+\nu_e$) [16]	(^{20}Ne, $n\gamma$) [17,18]	(p, d) [19]	(^{3}He, t) present	E_x adopted	J^π; T adopted	Γ_{p_0}/Γ	$\Gamma_{p_{1,2}}/\Gamma$
[7888(25)]		7882(15)		7912(5)[b]	7894(3)	7893.5(29)	$(1/2^+, 3/2^+, 5/2^+)$	$0.97^{+0.12}_{-0.61}$	$0.13^{+0.03}_{-0.09}$
					7905(3)	7905(3)	$(1/2^+ - 13/2^-)$	$0.34^{+0.12}_{-0.29}$	<0.03
					7932(3)	7932(3)	$(1/2^+ - 13/2^-)$	$1.22^{+0.18}_{-0.69}$	<0.04
					7945(3)	7945(3)	$(1/2^+ - 13/2^-)$	$1.29^{+0.30}_{-0.95}$	<0.16
7985(25)					7973(3)	7973(3)	$(1/2^+ - 13/2^-)$; (3/2)	$0.62^{+0.11}_{-0.42}$	$0.70^{+0.09}_{-0.44}$
		8021(16)			8015(3)	8015.2(29)	$(1/2^+, 3/2^+, 5/2^+)$; (3/2)	$0.67^{+0.19}_{-0.52}$	$0.53^{+0.12}_{-0.38}$
					[8030(3)]	[8030(3)]	$(1/2^+ - 13/2^-)$	$1.18^{+0.16}_{-0.75}$	
				8049(6)	8044(3)	8045.0(27)	$(1/2, 3/2, 5/2)^+$	$0.66^{+0.11}_{-0.44}$	$0.95^{+0.10}_{-0.41}$
					[8060(3)]	[8060(3)]		<0.36	<0.62
[8082(25)]					8071(3)	8071(3)	$(1/2^+ - 13/2^-)$	$1.07^{+0.22}_{-0.75}$	<0.29
					[8106(10)]	[8106(10)]	$(1/2^+ - 13/2^-)$	$1.08^{+0.39}_{-0.93}$	$0.79^{+0.20}_{-0.59}$
					8131(3)	8131(3)	$\geqslant 1/2^-$	$0.71^{+0.13}_{-0.13}$	$0.05^{+0.02}_{-0.04}$
8183(25)				8171(12)	8178(3)	8177.7(29)	$(5/2^+ - 13/2^-)$	$1.00^{+0.15}_{-0.15}$	$0.13^{+0.04}_{-0.11}$
					[8209(3)]	[8209(3)]	$(1/2^+ - 13/2^-)$	<0.33	$0.13^{+0.05}_{-0.11}$
					8229(3)	8229(3)	$(1/2^+ - 13/2^-)$	$0.86^{+0.33}_{-0.55}$	$0.40^{+0.08}_{-0.28}$
		8296(21)			8268(10)[o]	8273(9)	$(1/2^+, 3/2^+, 5/2^+)$		$0.49^{+0.18}_{-0.43}$
					8330(8)[o]	8330(8)	$(1/2^+ - 13/2^-)$	$1.16^{+0.20}_{-0.78}$	$0.13^{+0.06}_{-0.12}$
8362(25)					8382(10)[o]	8379(9)	$(1/2^+ - 13/2^-)$	$0.90^{+0.14}_{-0.58}$	$0.16^{+0.02}_{-0.10}$
		8418(21)			8418(5)	8418(5)	$(1/2^+, 3/2^+, 5/2^+)$		
8453(25)			8461[p]		[i]	8461[p]	$13/2^-$		
		8509(16)		8517(13)	8498(5)	8501(5)	$1/2^+$		
					8562(8)	8562(8)			
		[8669(40)]			[i]	[8669(40)]	$(1/2^+, 3/2^+, 5/2^+)$		
				8789(6)	[i]	8789(6)	$(3/2, 5/2)^+$		
		[8821(40)]			8813(15)	8816(12)	$(1/2^+, 3/2^+, 5/2^+)$		
					8904(20)	8904(20)			
		[8977(40)]			8969(20)	8971(18)	$(1/2^+, 3/2^+, 5/2^+)$		
					9004(20)	9004(20)			
					9077(20)	9077(20)			
			9154.0(12)		9151(25)	9154.0(12)	$13/2^+$		
				9207(5)	9190(25)	9206(5)			
					9226(25)	9226(25)			
					9332(30)	9332(30)			
				9423(7)	9398(30)	9422(7)	$(3/2, 5/2)^+$		
				9606(14)	[q]	9606(14)			
				9853(12)	[q]	9853(12)			
			10146.0(10)		[q]	10146.0(10)	$15/2^-$[r]		
				10577(13)	[q]	10577(13)			

[a]Constrained by available ^{31}P mirror levels, assuming a complete ^{31}P level scheme.
[b]Not used in adopted-energy average.
[c]Used in energy calibration.
[d]Determined using ^{27}Si calibration independently of Ref. [18].
[e]Observed, but peak position held fixed in focal-plane multiplet fit [20].
[f]Derived from averaging 6401(3) and 6398(6) keV from the present (^{3}He, t) and (d, t) measurements, respectively.
[g]Lower limit due to possible detection-threshold effects.
[h]Assuming 100% proton-detection efficiency at all YLSA angles (near energy threshold).
[i]Not observed in the present work.
[j]Assuming $J^\pi = 11/2^-$, 6833.4-keV level is relatively weakly populated. Derived from averaging 6836(2) and 6837(7) keV from the present (^{3}He, t) and (d, t) measurements, respectively.
[k]Lower limit assuming $J^\pi = 11/2^-$, 6833.4-keV level not populated.
[l]Modified from Refs. [14,15] after Ref. [35].
[m]Reference [36] to omit Ref. [37] measurement, which is included in 7156(5) keV in next column.
[n]Implied by 1004-keV γ-ray feeding the 6636.3(15) keV, $J^\pi = 9/2^-$ level [18]. Uncertainty not published, but is likely $\lesssim$2 keV.
[o]Inflated uncertainty because extrapolation of 20-MeV energy calibration was used.
[p]Uncertainty not published, but is likely $\lesssim$2 keV.
[q]Not observed ($\rho < 70$ cm: off focal plane detector).
[r]Originally assigned $J^\pi = (13/2)^-$ in Ref. [17] but modified in Ref. [38] after Ref. [39].

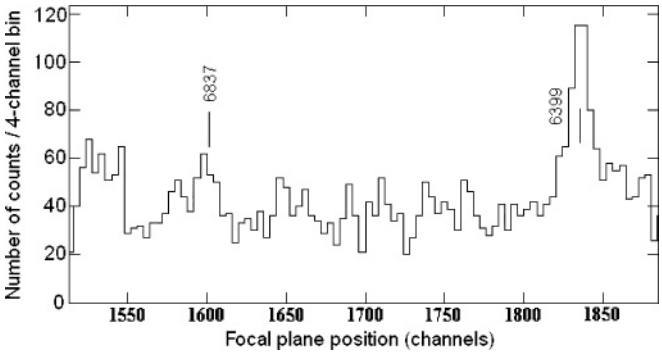

FIG. 7. Triton focal-plane position spectrum of the ^{32}S$(d, t)^{31}$S reaction using a 25-MeV deuteron beam at $\theta_{\rm lab} = 20^\circ$ and an aperture setting of $\Delta\theta = \pm 10$ mrad. The histogram is plotted in bins of four channels, and shows only the region of astrophysical interest.

position were derived at each angle ($0.29 \leqslant \chi^2_\nu \leqslant 1.76$). Excitation energies are reported for two levels of astrophysical interest, and are averaged with the (^{3}He, t) values, in Table I (see footnotes f and j). Background and poor statistics limited the number of levels that could be detected, and precluded a meaningful DWBA analysis to constrain spins. An embedded ^{32}S target might yield cleaner spectra for future measurements.

IV. DISCUSSION

A. Energy levels of ^{31}S

At all angle/beam-energy combinations, the nonselective (^{3}He, t) reaction populated most known ^{31}S states, reducing many excitation-energy uncertainties above $E_x = 4.9$ MeV. In general, the level energies are in excellent agreement with those from previous work. The level scheme of ^{31}S has also been considerably extended. As discussed in our previous publication [20], new levels were found at $E_x = 6134$, 6327, and 6399 keV, and a tentative level at 6585 keV was confirmed. In the present work, we report 14 additional new levels and 5 tentative new levels. We also confirm 5 tentatively known levels (Table I). Most excitation energies have been determined to ± 3 keV or better up to 8.25 MeV. Above this energy, uncertainties range from 5 keV to 30 keV due to uncertainties in the focal-plane calibrations. The experimentally measured ^{31}S-^{31}P mirror-level densities are now comparable up to 8.4 MeV, but the sparsity of the ^{31}S level scheme above 8.4 MeV indicates that it remains incomplete at higher energies. Finite proton-decay branching ratios to the ground state of ^{30}P have been measured for the first time for 35 levels, and upper limits have been set for 5 additional levels. The sum of the proton-decay branching ratios to the first two excited states of ^{30}P has been determined for the first time for 13 levels, and upper limits have been set for 15 additional levels. A total of 18 angular-correlation measurements have been made for 17 levels; 8 of these displayed significant anisotropy leading to a measured spin-parity constraint. The lowest isospin $T = 3/2$ level has been measured, and several candidates for the second and third isospin $T = 3/2$ levels have been identified. The Appendix contains an extensive discussion of the measured properties of individual levels, and the results are summarized in Table I.

With the ultimate goal of deriving a thermonuclear ^{30}P$(p, \gamma)^{31}$S reaction rate over a broad range of temperatures, we systematically evaluated ^{31}S levels as ^{30}P + p resonances. Constraints on J^π values from our coincidence measurements are discussed in the Appendix, where a ^{31}P mirror level is selected to pair with most ^{31}S levels up to $E_x = 8379$ keV ($E_r = 2246$ keV) to further constrain J^π (and Γ_γ where possible). Figure 8 depicts the level schemes of ^{31}S and ^{31}P, with possible mirror assignments, over the energy range $6700 < E_x(^{31}\text{S}) < 7200$ keV; similar diagrams for lower excitation energies can be found in Refs. [20,25]. In a few cases, where a mirror partner with similar excitation energy and consistent J^π was not available, we appealed to sd shell-model predictions [24,35]. By necessity, a significant component of this procedure was based on arbitrary choices, and in some cases the J^π values used were completely arbitrary. *Unless otherwise indicated in Table* I, *the* J^π *values used for the rate calculation in the present work are (at best) educated guesses and are not intended to be firm assignments.* Correct individual J^π values are less critical to the evaluation of the high-energy resonance strengths because $\Gamma_p \gg \Gamma_\gamma$ for most high-energy resonances, and we have data on the proton branching ratios; this information removes the requirement for a J^π-dependent calculation of Γ_p [Eq. (4)].

B. Astrophysical implications

Adopting the ^{31}S excitation energies from Table I, the Q value of 6133.0(15) keV [13], and the J^π values discussed above (and in the Appendix), the resonant ^{30}P$_{\rm g.s.}(p, \gamma)^{31}$S reaction rate was calculated under the narrow-resonance formalism [Eq. (1)] using resonances with $E_r \leqslant 2246$ keV.

For $T > 1$ GK, the thermal populations of excited states in ^{30}P are expected to be significant and this can be accounted for by using the stellar enhancement factors from Ref. [12]. In fact, the finite $p_{1,2}$ branching ratios measured in the present work provide the first direct experimental indications of resonances that may contribute significantly to the thermonuclear proton-capture rate on the first two excited states of ^{30}P. However, we do not attempt to apply this information to calculations of these rates because the p_1 decays were not resolved from the p_2 decays, and because there is a good chance that resonances below our proton-detection threshold would also make major contributions to these rates.

For Γ_{p_0}/Γ we used the values measured in the present work. If the value was greater than unity, we used the physical value of unity. For resonances where only an upper limit on Γ_{p_0}/Γ was extracted, we used the 90% C.L. upper limit from the present work. For levels where no information on Γ_{p_0}/Γ was extracted, proton widths were estimated using the formula [8]

$$\Gamma_p = \frac{2\hbar^2}{\mu R_n^2} P_\ell(E_r, R_n) C^2 S \theta^2_{\rm s.p.}, \qquad (4)$$

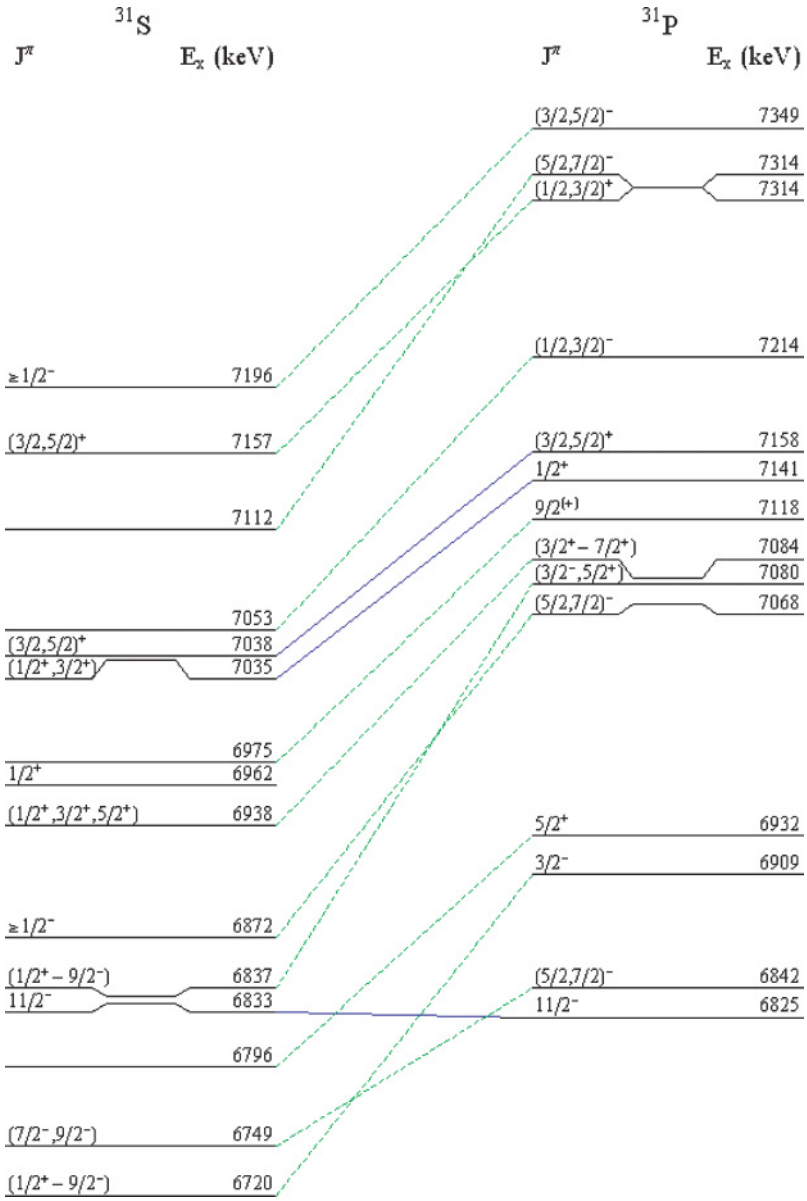

FIG. 8. (Color online) Level structures of ^{31}S and ^{31}P for $6700 < E_x(^{31}\mathrm{S}) < 7200$ keV, labeled by the presently adopted J^π values and excitation energies for ^{31}S (Table I), and values from Refs. [14,15,17,18,35] for ^{31}P. Solid (blue online) lines indicate mirror assignments from Refs. [14,15,17,18,35]. Dashed (green online) lines indicate possible additional mirror assignments that are used to derive ^{31}S J^π values for the rate calculation in the present work. A discussion is available in the Appendix.

where $R_n = 1.25(1^{1/3} + 30^{1/3})$ fm is the interaction radius, $P_\ell(E_r, R_n) \equiv kR_n/(F_\ell^2 + G_\ell^2)$ is the penetration factor[3] that was calculated by computing the regular (F_ℓ) and irregular (G_ℓ) Coulomb wave functions [8,40], C is an isospin Clebsch-Gordan coefficient, S is the spectroscopic factor, k is the wave number, and $\theta^2_{\mathrm{s.p.}}$ is the single-particle reduced width that was estimated using Ref. [41]. Following Refs. [18,19] we assumed $C^2S = 0.02$ for odd-parity resonances; we assumed $C^2S = 0.10$ for even-parity resonances.

For Γ_γ we adopted the value of the ^{31}P mirror level when it was known. Unfortunately, Γ_γ are only known for a handful of ^{31}P levels at these high excitation energies. For resonances where no direct mirror information was available we followed Ref. [18] and assumed $\Gamma_\gamma = 0.15$ eV for $E_r \leqslant 616$ keV based on the known lifetime of the 6909 keV ^{31}P level. For $E_r \geqslant 979$ keV we assumed $\Gamma_\gamma = 0.55$ eV based on the known lifetimes of the 7214 and 7314 keV ^{31}P levels. For $616 < E_r < 979$ keV, Γ_γ was increased linearly with energy from 0.15 to 0.55 eV, and rounded to a 100 meV increment. Considering Γ_γ to be a function of excitation energy in this way is a gratuitous oversimplification. However, our aim is to use experimental information on ^{31}S and ^{31}P wherever possible in keeping with previous experimental estimates [18,19] so that the results can be compared with HF calculations. This procedure would benefit from more experimental information on ^{31}P (or ^{31}S) levels at high excitation energies that would allow Γ_γ to be estimated on a level-by-level basis. Shell-model estimates of Γ_γ are complicated by the high excitation energies of the levels involved, and would require the use of a shell-model Hamiltonian comprising both the sd and fp shells.

[3]Equation (4) is identical to that used in Ref. [20], but the more modern definition of the penetration factor (with a factor kR_n absorbed) is adopted in the present work.

TABLE II. ^{30}P$(p,\gamma)^{31}$S resonance parameters used for the rate calculation of Table III; details are available in the text. For $6.1 < E_x < 6.7$ MeV see Ref. [20]. For $E_x > 7.2$ MeV see Table I and the Appendix. The J^π values in square brackets should not be interpreted as true J^π constraints; the experimental J^π constraints are summarized in Table I.

E_x (keV)	E_r (keV)	J^π	ℓ	$\theta_{\text{s.p.}}$	C^2S	Γ_p (keV)	Γ_p/Γ	Γ_γ (keV)	$\omega\gamma$ (keV)
6719.8(20)	586.8(25)	$[3/2^-]$	1				$0.25^{+0.07}_{-0.20}$	1.5×10^{-4}	2.50×10^{-5}
6749.0(20)	616.0(25)	$[7/2^-]$	3				$0.57^{+0.07}_{-0.32}$	1.5×10^{-4}	1.14×10^{-4}
6796(25)	663(25)	$[5/2^+]$	2	0.36	0.10	4.38×10^{-4}		2.0×10^{-4}	1.37×10^{-4}
6833.4(3)	700.4(15)	$11/2^-$	5	1.00	0.02	2.88×10^{-9}		$5.4(22) \times 10^{-6}$	5.77×10^{-9}
6836.5(18)	703.5(23)	$[3/2^-]$	1				$0.48^{+0.07}_{-0.34}$	3.0×10^{-4}	9.60×10^{-5}
6872.0(20)	739.0(25)	$[7/2^-]$	3				$0.37^{+0.09}_{-0.13}$	3.0×10^{-4}	1.48×10^{-4}
6938.1(29)	805.1(32)	$[3/2^+]$	0				1.00[a]	4.0×10^{-4}	2.67×10^{-4}
6962.3(26)	829.3(30)	$1/2^+$	0				$0.46^{+0.11}_{-0.40}$	4.0×10^{-4}	6.13×10^{-5}
[6975(3)]	[842.0(34)]	$[9/2^+]$	4				0.38[b]	4.0×10^{-4}	2.53×10^{-4}
7035.4(20)	902.4(25)	$(1/2^+)$	0				1.00[a]	$2.0(2) \times 10^{-3}$	6.63×10^{-4}
7038(4)	905.0(43)	$5/2^+$	2	0.36	0.10	5.99×10^{-3}		5.0×10^{-4}	4.61×10^{-4}
[7053.0(20)]	[920.0(25)]	$[1/2^-]$	1				$0.36^{+0.15}_{-0.33}$	$5.7(11) \times 10^{-4}$	6.80×10^{-5}
7112(25)	979(25)	$[7/2^-]$	3	0.35	0.02	9.77×10^{-5}		5.5×10^{-4}	1.11×10^{-4}
7156.5(17)	1023.5(23)	$[3/2^+]$	0				1.00[a]	$5.5(7) \times 10^{-4}$	3.66×10^{-4}
7196.1(20)	1063.1(25)	$[3/2^-]$	1				$0.67^{+0.08}_{-0.12}$	5.5×10^{-4}	2.46×10^{-4}

[a]Physical value of unity used because measured value is greater than unity.
[b]90% C.L. upper limit used.

Resonance parameters for $E_r \leqslant 504.0$ keV are summarized in Table II of Ref. [20]. In addition, we tabulate the resonance parameters used for $504.0 < E_r \leqslant 1063.1$ keV in Table II of the present work. For the many resonances in the range $1063.1 < E_r \leqslant 2246$ keV, we simply use Γ_p/Γ from Table I and $\Gamma_\gamma = 0.55$ eV, with the spin assumptions outlined in the Appendix. Undoubtedly many of the specific spin assumptions are incorrect but the overall distribution of spins used is roughly correct and, statistically, we expect this to provide a useful determination of the high-temperature rate when the contributions from all resonances are summed. The reaction rate is tabulated in Table III.

The salient features of the reaction rate for $0.1 < T < 0.4$ GK were discussed in our earlier publication [20]. Briefly, the new resonances at $E_r = 194.0$ and 266.4 keV increased the experimentally determined reaction rate by up to an order of magnitude in this range. As shown in Fig. 9 the reaction rate is up to a factor two larger than that from Refs. [18,19] for $0.4 < T < 1.0$ GK. Above 1 GK, an experimentally determined reaction rate has only been previously reported in

TABLE III. Thermonuclear, resonant ^{30}P$(p,\gamma)^{31}$S reaction rate $N_A\langle\sigma\upsilon\rangle_{\text{g.s.}}$ in cm^{3}mol^{-1}s^{-1}.

T(GK)	$N_A\langle\sigma\upsilon\rangle_{\text{g.s.}}$	T(GK)	$N_A\langle\sigma\upsilon\rangle_{\text{g.s.}}$	T(GK)	$N_A\langle\sigma\upsilon\rangle_{\text{g.s.}}$	T(GK)	$N_A\langle\sigma\upsilon\rangle_{\text{g.s.}}$
0.01	1.64×10^{-36}	0.17	2.16×10^{-6}	0.34	1.61×10^{-2}	0.8	2.71×10^{1}
0.015	3.32×10^{-32}	0.18	4.48×10^{-6}	0.35	2.29×10^{-2}	0.85	3.91×10^{1}
0.02	4.15×10^{-30}	0.19	8.82×10^{-6}	0.36	3.20×10^{-2}	0.9	5.46×10^{1}
0.03	4.92×10^{-25}	0.20	1.66×10^{-5}	0.37	4.40×10^{-2}	0.95	7.43×10^{1}
0.04	6.88×10^{-20}	0.21	3.03×10^{-5}	0.38	5.95×10^{-2}	1.0	9.85×10^{1}
0.05	7.94×10^{-17}	0.22	5.40×10^{-5}	0.39	7.93×10^{-2}	1.5	6.72×10^{2}
0.06	8.68×10^{-15}	0.23	9.48×10^{-5}	0.40	1.04×10^{-1}	2.0	1.84×10^{3}
0.07	2.70×10^{-13}	0.24	1.64×10^{-4}	0.42	1.73×10^{-1}	3.0	4.91×10^{3}
0.08	4.41×10^{-12}	0.25	2.82×10^{-4}	0.44	2.76×10^{-1}	4.0	7.77×10^{3}
0.09	5.00×10^{-11}	0.26	4.76×10^{-4}	0.46	4.23×10^{-1}	5.0	1.00×10^{4}
0.10	4.13×10^{-10}	0.27	7.92×10^{-4}	0.48	6.25×10^{-1}	6.0	1.16×10^{4}
0.11	2.53×10^{-9}	0.28	1.29×10^{-3}	0.5	8.97×10^{-1}	7.0	1.26×10^{4}
0.12	1.19×10^{-8}	0.29	2.07×10^{-3}	0.55	1.99×10^{0}	8.0	1.32×10^{4}
0.13	4.49×10^{-8}	0.30	3.26×10^{-3}	0.6	3.88×10^{0}	9.0	1.35×10^{4}
0.14	1.42×10^{-7}	0.31	5.01×10^{-3}	0.65	6.93×10^{0}	10.0	1.36×10^{4}
0.15	3.92×10^{-7}	0.32	7.55×10^{-3}	0.7	1.15×10^{1}		
0.16	9.62×10^{-7}	0.33	1.11×10^{-2}	0.75	1.81×10^{1}		

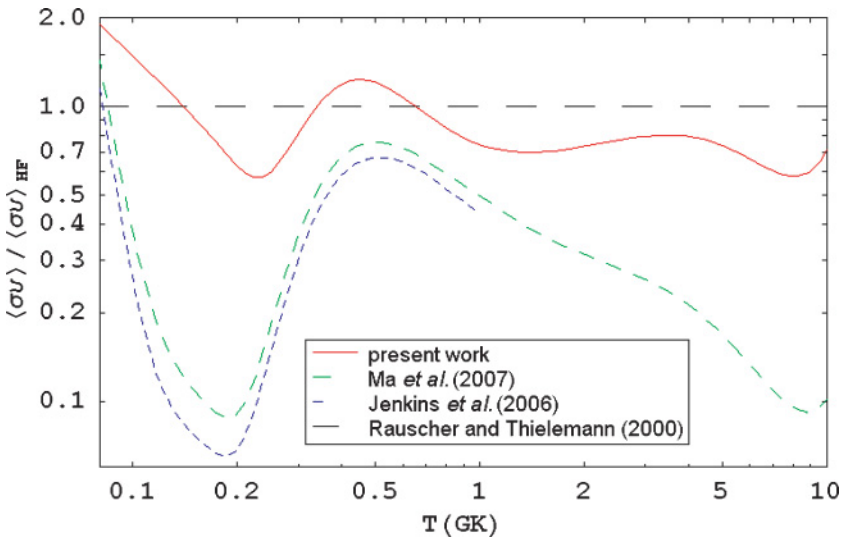

FIG. 9. (Color online) Ratios of the experimentally based, resonant ^{30}P$(p,\gamma)^{31}$S reaction rates derived in the present work, the work of Jenkins *et al.* [18], and the work of Ma *et al.* [19] to the rate from the Hauser-Feshbach calculations of Rauscher and Thielemann [12].

Ref. [19]. We find our reaction rate to be up to a factor seven larger than that in Ref. [19] for $T > 1$ GK. The difference can be attributed to three major factors: (1) new resonances discovered in the present work, (2) inclusion of a broader range of resonance energies in the present work, and (3) larger values of Γ_γ used in the present work for higher-energy resonances. As shown in Fig. 9, the reaction rate calculated in the present work is in agreement with HF estimates [12] within their stated level of accuracy (a factor two for $T >$ 0.24 GK) over the broader temperature range $0.08 < T <$ 10.00 GK. It is possible that our reaction rate at higher temperatures is deficient due to a yet-incomplete ^{31}S level scheme or unaccounted-for contributions from broad resonances. Direct measurements [42] of the ^{30}P$(p,\gamma)^{31}$S excitation function using a ^{30}P beam could improve upon these uncertainties, and on the uncertainties in the rate at all temperatures. Additional suggestions for future work may be found in Ref. [25].

V. CONCLUSIONS

The nonselective $(^3\mathrm{He}, t)$ reaction has been exploited, together with coincidence techniques and the (d, t) reaction to derive a ^{31}S level scheme up to $E_x = 9.5$ MeV, with similar density to that of its mirror, ^{31}P, up to $E_x = 8.4$ MeV. Using this new information yields an experimentally determined thermonuclear ^{30}P$(p,\gamma)^{31}$S reaction rate that is in much better agreement with Hauser-Feshbach statistical-model estimates than with previous experimental determinations. The reaction rate from the present work may be used in astrophysical models of ONe novae, rp-process nucleosynthesis, and oxygen burning in massive stars. The new information on ^{31}S levels will also facilitate direct studies of $^{30}\mathrm{P} + p$ resonances using radioactive ^{30}P beams.

ACKNOWLEDGMENTS

We gratefully acknowledge A. Champagne, C. Westerfeldt, and J. Wilkerson for contributing to the target preparation. We thank W. Bradfield-Handler, R. Lewis, T. Rounsaville, D. Visser, and the WNSL staff for their contributions at Yale. We also appreciate the insightful suggestions of A. Champagne, A. Heinz, D. Hutcheon, F. Iachello, C. Iliadis, S. Lamoreaux, and V. Werner. Funding was provided the US Department of Energy, Office of Nuclear Physics, under Grant Nos. DE-FG02-91ER40609 and DE-FG02-97ER41020.

APPENDIX: DISCUSSION OF INDIVIDUAL ^{31}S ENERGY LEVELS AS $^{30}\mathrm{P} + p$ RESONANCES

Subthreshold levels. All 12 known levels with $4.9 < E_x < 6.1$ MeV (below the proton threshold of $E_x =$ 6133 keV) were populated. There was no evidence for additional levels or background peaks (Fig. 3C). The excitation-energy uncertainties were reduced considerably. We include the results of excitation-energy measurements for subthreshold levels in Table I. J^π values for subthreshold levels from previous measurements are also compiled. Spins for the 5024-, 5405-, 5439-, 5678-, and 5824-keV levels have been constrained by assuming completeness of the ^{31}P level scheme in this energy region and determining possible mirror assignments based on previously unpaired levels with similar excitation energies. The energy of the known 5978.2(7)-keV level was used as an internal focal-plane calibration point. Notably, there exists one ^{31}P level without a mirror partner due to the apparent ^{31}P doublet at 5892 keV [35]. It is, therefore, possible that one of the ^{31}S levels in this energy region is an unresolved doublet.

6134-6637 keV. Our results in this energy range were discussed in an earlier publication [20], where all nine known levels and three new levels were reported to have been excited. Our excitation of 21 out of 21 known levels, regardless of spin or isospin, for $4.9 < E_x < 6.7$ MeV demonstrates the nonselectivity of the ^{31}P$(^3\mathrm{He}, t)$ reaction and warrants reexamination of levels with $E_x > 6.7$ MeV observed in other work that are not observed in the present work. The 6399-keV level was also measured to have $E_x = 6398(6)$ keV using the (d, t) reaction (Fig. 7). Among these levels, the 6160.2(7) and

6636.3(15)-keV levels were used as internal energy-calibration points. Spins, parities, and energies are summarized in Table I.

The present article affords some elaboration on the analysis of the 20-MeV (^{3}He, t) singles spectra that led to the determination of a new level at 6401(3)-keV in Ref. [20]. In particular, it is important to note that when none of the peak positions were constrained, sufficiently good fits to the spectra in the range $6.2 < E_x < 6.5$ MeV were obtained using only 6 peaks (rather than seven, as shown in Fig. I in Ref. [20]). Considering that the precise excitation energies of the $9/2^-$, 6376.9(5)-keV and $11/2^+$, 6393.7(5)-keV levels were measured in the same experiment [17,18] as the precise energies of the internal-calibration points used in the present experiment, we expected the internal calibrations of the (^{3}He, t) spectra to yield consistent energies for the 6376.9- and 6393.7-keV levels. However, using the internal calibration points and the 6-peak fits instead led to excitation energies for the 6376.9- and 6393.7-keV levels that were higher than the previously measured energies by nearly 4 keV in each spectrum. Another measurement [38,43] of $E_x = 6391.1(12)$ keV for the $11/2^+$ level compounded this discrepancy, and persuaded us to constrain the positions of the 6376.9- and 6393.3-keV peaks in the fits, each of which then required a 7th peak with reasonably high confidence corresponding to the new 6401(3)-keV level. The confidence levels quoted in Ref. [20] for the detection of a new level at 6401(3) keV are based entirely on these constrained fits. In nuclear spectroscopy, it is usually the case that the accuracies of excitation-energy measurements are dependent on the accuracies of calibration energies that are adopted from other publications. In the present case, the very *existence* of the 6401(3) keV peak is dependent on the accuracies of the precise calibration energies from Refs. [17,18,38,43]. Higher-resolution measurements of the ^{31}P(^{3}He, t)^{31}S reaction in this energy range could be used to search for the 6401(3)-keV peak independently of calibration data; such measurements are already planned [44] for the Q3D spectrograph at the Maier-Leibnitz Laboratory in Garching. The statistical verification of all other peaks reported in Ref. [20] and herein was done independently of calibration data.

6720 keV. Under the assumption of 100% detection efficiency, this level exhibits a p_0 branching of $0.25^{+0.07}_{-0.20}$. However, the branching ratio should be conservatively considered as a lower limit due to the proximity of this level to the proton-detection threshold. Because of the finite proton branch, we constrain $J^\pi = (1/2^+ - 9/2^-)$. Based on possible mirror levels at $[E_x(^{31}\mathrm{P});\ J^\pi] = [6842\ \mathrm{keV},\ (5/2, 7/2)^-]$, [6909 keV, $(3/2^-)$], [6932 keV; $(5/2^+)$], it likely has $J^\pi = (3/2^-, 5/2, 7/2^-)$. For the rate calculation, our choice of the [6909 keV, $3/2^-$] ^{31}P level to be the mirror of this state is influenced by our mirror assignment for the 6749 keV ^{31}S level.

6749 keV. The $n \leqslant 4$ fit to the t-p angular correlation of this level yielded a p value of 0.046 and this suggests $\ell_{\mathrm{min}} = 3$. However, one cannot make a meaningful least-squares $n \leqslant 6$ fit (with 4 free parameters) to 4 data points to determine the branching ratio, and the isotropic fit was not substantially worse than the $n \leqslant 2$ fit, so we used the isotropic distribution (Fig. 6) to determine a branching ratio of $0.57^{+0.07}_{-0.32}$. Using the constraint $J^\pi = (7/2^-, 9/2^-)$ from the $\ell_{\mathrm{min}} = 3$ measurement suggests that the most reasonable mirror level is at $[E_x(^{31}\mathrm{P});\ J^\pi] = [6842\ \mathrm{keV},\ (5/2, 7/2)^-]$. Adopting this mirror assignment and the measured constraint results in $J^\pi = 7/2^-$ for the rate calculation. It should, however, be noted that the low coincidence rate observed at the most backward angle strongly influences the fit of this angular correlation, but may be a statistical (or threshold) anomaly since anisotropic angular correlations are generally peaked at 180° (Fig. 6).

6796 keV. This level has only been observed in a ^{29}Si(^{3}He, n) study [45] with 25-keV uncertainty, and we do not observe a level in 1σ agreement with this energy. Based on possible mirror levels at $[E_x(^{31}\mathrm{P});\ J^\pi] = [6842\ \mathrm{keV},\ (5/2, 7/2)^-]$, [6909 keV, $(3/2^-)$], and [6932 keV; $(5/2^+)$], it likely has $J^\pi = (3/2^-, 5/2, 7/2^-)$. For the rate calculation we choose the [6932 keV; $(5/2^+)$] level and assume $J^\pi = 5/2^+$ because the other two mirror possibilities are connected to the 6749 and 6720 keV ^{31}S levels, and because the ^{29}Si(^{3}He, n) reaction is known to excite other $J^\pi = 5/2^+$ levels [45].

6833 and 6837 keV. Surprisingly, we observed a significant proton branch from a peak with an energy of 6836(2) keV, nearly degenerate with the known $J^\pi = 11/2^-$ level [17,18] at 6833.4(3) keV (we do not expect the corresponding $\ell = 5$ proton decay to compete with γ decay at this low proton energy). This observation and expectation appear to necessitate a doublet near this energy, and therefore this potentially excellent internal energy calibration point was not used for that purpose. Our angular-correlation fit method narrowly deduces $\ell_{\mathrm{min}} = 0$ based on our p-value guidelines, but the p value of 0.053 for the isotropic fit is somewhat suggestive of higher-order terms (Fig. 6). The spin of the new level is thus constrained to be $J^\pi = (1/2^+ - 9/2^-)$, with $J^\pi = (1/2^- - 9/2^-)$ most likely. Using available mirror levels at $[E_x(^{31}\mathrm{P});\ J^\pi] = [7068\ \mathrm{keV};\ (5/2, 7/2)^-]$, [7080 keV; $(3/2^-, 5/2^+)$], and [7084 keV; $(3/2^+ - 7/2^+)$], and assuming completeness of the ^{31}P level scheme we obtain a second constraint: $J^\pi = (3/2 - 7/2)$. For the rate calculation we choose the $[E_x(^{31}\mathrm{P});\ J^\pi] = [7080\ \mathrm{keV};\ (3/2^-, 5/2^+)]$ mirror partner and use $J^\pi = 3/2^-$ arbitrarily. This mirror assignment is linked to those for the 6872-keV and 6973-keV ^{31}S levels. Using the isotropic angular correlation yields a branching ratio of $0.48^{+0.07}_{-0.34}$; this should be considered a lower limit since we likely also populated the unresolved, γ-decaying, 6833-keV level in our triton-singles spectrum. A level was also measured to have $E_x = 6837(7)$ keV using the (d, t) reaction (Fig. 7) and we identify it with the level measured using the (^{3}He, t) reaction because we do not expect the (d, t) reaction to populate the $11/2^-$ level as strongly as a level with relatively low spin.

6872 keV. The angular-correlation measurements yielded p values <0.0001 and $= 0.016$ for the isotropic and $n \leqslant 4$ fits, respectively; this firmly determines $J^\pi \geqslant 1/2^-$ and strongly suggests $J^\pi = (7/2^-, 9/2^-)$. Considering the possible mirror levels at $[E_x(^{31}\mathrm{P});\ J^\pi] = [7068\ \mathrm{keV};\ (5/2, 7/2)^-]$, [7080 keV; $(3/2^-, 5/2^+)$], and [7084 keV; $(3/2^+ - 7/2^+)$], we match it with the [7068 keV; $(5/2, 7/2)^-$] level and assume $J^\pi = 7/2^-$ for the rate calculation based on these constraints. Because we cannot use an $n \leqslant 6$ fit to determine a meaningful branching

ratio, and because the $n \leqslant 2$ fit is as good as (and simpler than) the $n \leqslant 4$ fit, we use the $n \leqslant 2$ fit (Fig. 6) to determine $\Gamma_p/\Gamma = 0.37^{+0.09}_{-0.13}$.

6938, 6962, [6975] keV. Three levels at 6939(3), 6961(3), and [6975(3)] keV are needed to fit this broad, irregular peak (Fig. 3) sufficiently well in the high-statistics spectra. An uncertainty of 3 keV was assigned rather than 2 keV because the presence of three constituent peaks was only statistically significant in the high-statistics spectra, and this resulted in a relatively large reproducibility uncertainty (only the forward-angle measurements were used to determine the reported energies). The low-statistics spectra were fit sufficiently well by two peaks. There is an asymmetry in the proton branching of the total peak, with stronger proton decay weighted to the low excitation-energy side.

A meaningful angular correlation could only be obtained for the 6962-keV level; a p value of 0.118 was determined for the isotropic fit, yielding $\ell_{\min} = 0$, which is somewhat suggestive of higher-order terms but not definitive in this respect (Fig. 6). The isotropic fit is sufficient by our guidelines, and is consistent with the previous $J^\pi = 1/2^+$ assignment for the known 6966(5)-keV level [35]. Besides the $J^\pi = (1/2, 3/2)^+$ ^{31}P level at 7314 keV [which seems to match better with the $J^\pi = (3/2, 5/2)^+$, 7157 keV ^{31}S level], there is no candidate ^{31}P mirror level. Therefore we identify this level with the unpaired $1/2^+_6$, shell-model level that is expected at 7346 keV [24,35] for the rate calculation.

If we tentatively identify the 6938-keV level with the $J^\pi = (1/2^+, 3/2^+, 5/2^+)^*$ ^{31}S level inferred[4] at 6921(13)* keV from ^{31}Cl β^+-delayed proton-decay measurements [16], then the only consistent ^{31}P mirror level remaining is $[E_x(^{31}\mathrm{P}); J^\pi] = [7084\ \mathrm{keV}; (3/2^+ - 7/2^+)]$. For the rate calculation we narrow the spin-parity to $J^\pi = (3/2, 5/2)^+$ based on the constraints discussed, and choose $3/2^+$ arbitrarily.

Finally, the [6975]-keV level does not have a large proton-decay branch, so it is natural to pair it with the [7084 keV; $9/2^{(+)}$] ^{31}P level for the rate calculation, because we expect the $\ell = (4)$ proton branch to be small. Because of the unobserved proton-decay branch for this level, and the definitive observation of three constituent levels in this peak only at the most forward angles, we classify this level as tentative. Excluding this level from the fits would shift the energies of the 6938- and 6962-keV levels upward by 5 to 10 keV.

7006 keV. Although population of this second $T = 3/2$ level is isospin permitted in the $(^3\mathrm{He}, t)$ reaction, we do not observe a level with an energy in 1σ agreement with this previously measured 7006(25) keV, $J^\pi = 1/2^+$ level [45]. It has been observed only in a ^{29}Si$(^3\mathrm{He}, n)$ study [45] and its population is isospin forbidden in exhaustively studied single-neutron pickup reactions on ^{32}S. The small proton-branching ratio of the [6975]-keV level observed in the present work could be considered to be evidence for an identification with the $T = 3/2$ level because the proton decay of a $T = 3/2$ ^{31}S level to the $T = 0$ ground state of ^{30}P is isospin forbidden. However we find somewhat stronger evidence for identification with the 7036(2)-keV level observed in the present work, as discussed in the following paragraph.

7035, 7038, and [7053] keV. A known level at 7039(10) keV was assigned $J^\pi = (3/2, 5/2)^+$ in a 1998 compilation [14]. In more recent DWBA studies of the ^{32}S$(^3\mathrm{He}, \alpha)$ [35] and ^{32}S(p, d) [19] reactions that clearly yielded $\ell_n = 2$ for the transferred neutron, the $J^\pi = (3/2, 5/2)^+$ assignment was confirmed and the level was identified with the $5/2^+_9$ shell-model level [24,35] and the 7158 keV, $J^\pi = (3/2, 5/2)^+$ ^{31}P mirror. We observe a broad, intense peak (Fig. 3) around this energy that proton decays ≈100%, isotropically with higher-order angular-correlation terms that are consistent with zero (Fig. 6), suggestive of $J^\pi = (1/2^+, 3/2^+)$. Three possible explanations for the inconsistency in spin-parity between the present measurement and Ref. [35] are (1) the same $J^\pi = 5/2^+$ level is being observed but the higher-order angular-correlation terms are highly suppressed in the present work, (2) the $J^\pi = 5/2^+_9$ shell-model identification [35] is incorrect and the same $J^\pi = 3/2^+$ level is being observed, or (3) the $T = 3/2$, $J^\pi = 1/2^+$ level previously measured at 7006(25) keV [45] is nearly degenerate with the $5/2^+$ level, dominates the peak in the present work, and has a strong isospin-forbidden $\ell = 0$ proton decay to the $T = 0$ ^{30}P ground state (such isospin-forbidden decays are not uncommon [46,47]). The first possibility seems unlikely because this angular correlation has the highest statistics of any level, yet does not display any indication of anisotropy, in contrast to other levels with high statistics (Fig. 6). Regarding the second possibility: a large neutron spectroscopic factor was measured in Refs. [19,35], and is not predicted by the shell model for any $J^\pi = 3/2^+$ ^{31}S levels above the 1st excited state [24,35], so we see no reason to reject the $J^\pi = 5/2^+$ assignment for the level observed in the neutron-transfer experiments. Regarding the third possibility: we expect the 2nd $T = 3/2$ level to lie at roughly $6281 + 756 \approx 7040$ keV based on the energy of the first $T = 3/2$ ^{31}S level and the average difference in energy between the 1st and 2nd $T = 3/2$ levels in ^{31}P and ^{31}Si [14]. In addition, the ^{31}P$(^3\mathrm{He}, t)^{31}$S reaction has been shown in the present work to be almost absolutely nonselective in the levels it populates independently of spin, parity or isospin: therefore we expect to populate the 2nd $T = 3/2$ level significantly. This evidence appears to necessitate a doublet, and we tentatively conclude that the peak we measure at 7036(2) keV is predominantly populated by the $T = 3/2$, $J^\pi = 1/2^+$ level, in 1σ disagreement with the only other measurement of 7006(25) keV from ^{29}Si$(^3\mathrm{He}, n)$ studies. For the rate calculation, we use the measured 0.33(3)-fs lifetime [14] of the $T = 3/2$ analog level in ^{31}P to calculate $\Gamma_\gamma = 2.0$ eV.

There are two pieces of evidence for a new level at [7053] keV in the low-energy triton tail of this large peak. First,

[4]The excitation energy of this level (and for several other levels discussed hereafter) was derived under the assumption in Ref. [16] that all observed ^{31}Cl β^+-delayed proton decays are p_0. The $J^\pi = (1/2^+, 3/2^+, 5/2^+)$ assignment for this level (and for several other levels discussed hereafter) was derived under the assumption in Ref. [16] that all observed ^{31}Cl β^+ decays are allowed transitions. Hereafter, we denote level energies and spin constraints that were derived in this fashion with an asterisk *.

the total peak is broad and unusually asymmetric. Second, this portion of the peak is observed to have a deficient proton-decay branch relative to the bulk of the peak. The evidence is sufficient to tentatively deduce the existence of a new level at this energy. For the rate calculation we identify the new [7053]-keV level with the $[E_x(^{31}\mathrm{P});\ J^\pi] = [7214\ \mathrm{keV};\ (1/2, 3/2)^-]$ level based on similarity in excitation energy and arbitrarily choose $J^\pi = 1/2^-$. We use the measured $(2J+1)0.58(11)$-fs lifetime [14] of the analog level in ^{31}P to determine $\Gamma_\gamma = 0.57$ eV for the rate calculation. This level could also be considered to be a candidate for the second $T = 3/2$ level based on the small proton branching, but its energy is in nearly 2σ disagreement with the previous measurement of 7006(25) keV [45].

7112 keV. We did not observe the 7112(25)-keV level; it has only been populated using the ^{29}Si(^{3}He, n) reaction [45]. For the rate calculation we assign it to the $J^\pi = (5/2, 7/2)^-$ member of the ^{31}P doublet at 7314 keV and arbitrarily choose $J^\pi = 7/2^-$. This assignment is tied to the mirror assignments of the 7157- and 7196-keV ^{31}S levels; for these more information is available.

7157 keV. We observe a strong proton branch from this previously known [14] level with an angular correlation that is fit reasonably well by an isotropic fit (Fig. 6), yielding $\ell_{\min} = 0$. Using the constraint $\ell = (0, 2)$ from the compilation J^π value of $(3/2, 5/2)^+$ [14] yields a p_0 branching ratio $1.04^{+0.11}_{-0.63}$. The only known even-parity ^{31}P mirror level at a similar energy is the $J^\pi = (1/2, 3/2)^+$ member of the 7314-keV doublet. Identifying these levels with each other for the rate calculation requires $J^\pi = 3/2^+$ for both. A definitive $\ell = 0$ assignment would yield $\Gamma_p/\Gamma = 1.04^{+0.11}_{-0.11}$. We use the measured $(2J+1)0.30(4)$-fs lifetime [14] of the ^{31}P level to determine $\Gamma_\gamma = 0.55$ eV for the rate calculation.

7196 keV. The high statistics in the angular correlation for this previously known [14] level help us to firmly exclude the isotropic fit (p value <0.0001), and this firmly requires $J^\pi \geqslant 1/2^-$. However, it is fit reasonably well using $n \leqslant 2$ (Fig. 6), yielding $\ell_{\min} = 1$. The available mirror levels include $[E_x(^{31}\mathrm{P});\ J^\pi] = [7214\ \mathrm{keV};\ (1/2, 3/2)^-]$, [7314 keV; $(5/2, 7/2)^-$], and [7349 keV; $(3/2, 5/2)^-$]; this further constrains $J^\pi = (1/2 - 7/2)^-$ if we assume completeness of the ^{31}P level scheme. For the rate calculation we identify this level with the [7349 keV; $(3/2, 5/2)^-$] ^{31}P level because the $n = 4$ angular-correlation term was consistent with zero, and this is high-statistics case, which is suggestive of a $J^\pi = (1/2, 3/2, 5/2)^-$ assignment. We arbitrarily choose $J^\pi = 3/2^-$.

7303 keV. We populated this previously known [14,17,18] level and set a 90% C.L. upper limit of $\Gamma_p/\Gamma < 0.13$, consistent with the $J^\pi = 11/2^+$ assignment and strong γ decay observed in Refs. [17,18]. This level was used as an internal energy-calibration point.

7347 keV. The β^+-delayed proton decay of ^{31}Cl has been used previously [16,37] to infer the existence of energy levels in ^{31}S by assuming that p_0 emission absolutely dominates $p_{>0}$ emission. This assumption is contradicted by our observation of several $p_{1,2}$-decaying ^{31}S levels. Since the β^+-decay experiments had no means of discriminating proton decays to excited states in ^{30}P, it is likely that some of the ^{31}S-level energies inferred in these β^+-decay experiments were systematically in error by discrete amounts of $\Delta E_x(^{31}\mathrm{S}) = E_x(^{30}\mathrm{P}) = 677,\ 709,\ldots$ keV. For example, the existence of this $J^\pi = (1/2^+, 3/2^+, 5/2^+)^*$ ^{31}S level at 7347(14)* keV has been inferred from the observation of a 1174(14)-keV β^+-delayed proton-decay peak and was, at that time, identified [16] with a known 7310(11)-keV level [14,48] that is now known have $E_x = 7302.8(7)$ keV, $J^\pi = 11/2^+$ [18], and a very weak proton-decay branch $\Gamma_p/\Gamma < 0.13$ – all contradicting the β^+-decay identification. There is no evidence for a level near 7347 keV in other work, or in the present work despite the nonselective nature of the ^{31}P(^{3}He, t) reaction. We do, however, observe a peak at 8015(3) keV with $\Gamma_{p_{1,2}}/\Gamma = 0.53^{+0.12}_{-0.38}$ and propose the possibility that the 1174-keV β^+-delayed proton peak is from p_1 decay of this level. An 1826(15)-keV peak in the β^+-decay work corresponding to a ^{31}S excitation energy of 8021(16) keV (assuming p_0 decay) is likely due, at least in part, to the $\Gamma_{p_0}/\Gamma = 0.67^{+0.19}_{-0.52}$ branch of the 8015(3)-keV level observed in the present work. The $p_{1,2}$ branch that would result if the 1174- and 1826-keV β^+-delayed proton peaks were both from the same parent level can be calculated from Table 2 in Ref. [16] to be $\Gamma_{p_{1,2}}/\Gamma = 0.2(1)$, consistent with our measurement of $\Gamma_{p_{1,2}}/\Gamma = 0.53^{+0.12}_{-0.38}$ for the 8015-keV level. For these reasons we do not include the 7347(14)-keV ^{31}S level in our rate calculation.

7469 keV. Proton-decay statistics for this previously observed [14] level were not high enough to plot a meaningful angular correlation. By assuming an isotropic correlation we measured $\Gamma_{p_0}/\Gamma = 0.46^{+0.10}_{-0.33}$, inconsistent with unity. We would expect a value closer to unity for a low-spin level that is proton unbound by 1336 keV and, therefore, we expect this level to have a relatively high spin. The only mirror level in this excitation-energy region consistent with this expectation is the $J^\pi = (7/2, 9/2)^-$, 7466 keV ^{31}P level. We adopt this mirror assignment, and arbitrarily choose $J^\pi = 9/2^-$, for the rate calculation.

7501, 7519, and 7585 keV. These levels are all observed to have significant p_0-decay branches. The 7501-keV level has not been previously observed. We restrict the J^π values of the 7501- and 7585-keV levels to be $J^\pi = (1/2^- - 13/2^-)$ based on p values of 0.001 and 0.015, respectively, for the isotropic fits (Fig. 6), which yield $\ell_{\min} = 1$. Integrating the isotropic angular correlation for the 7519-keV level (Fig. 6) results in $\Gamma_{p_0}/\Gamma > 1$ so we tabulate the unconstrained value of $1.57^{+0.25}_{-0.97}$, with the central value obtained from the isotropic fit, and use the physical value of unity for the rate calculation. Possible mirror levels exist at (7687), 7715, 7736, and 7779 keV but several of these do not have well-defined spins. For the rate calculation, we pair the 7585-keV level with the $J^\pi = 3/2^-$ ^{31}P level at 7779 keV because this is consistent with the observed spin constraints, and adopt $J^\pi = 3/2^-$. We pair the 7501- and 7519-keV levels with the 7687- and 7715-keV levels in ^{31}P, respectively; these have unknown spins. Because the unpaired $5/2^+_{10}$ and $1/2^+_7$ shell-model levels are expected [24,35] to lie at 7641 and 7921 keV, respectively,

we use $J^\pi = 5/2^+$ and $1/2^+$ for the spins of the 7501- and 7519-keV levels, respectively, for the rate calculation.

7641 keV. We observe a 7641(3)-keV level with a small p_0 branch of $0.16^{+0.05}_{-0.13}$ (using an isotropic fit due to low statistics) that is suggestive of relatively high spin. Based on the finite proton branch we tentatively constrain $J^\pi = (1/2^+ - 13/2^-)$. We identify this level with a previously known [14] level at 7660(30) keV based on similar energies. This ^{31}S level can also be inferred from Ref. [18] where the mention of a 1004-keV γ-ray transition to the $J^\pi = 9/2^-$, 6636.3(15)-keV level implies a high-spin level at 7640.3 keV. Under the assumption that the 1004-keV radiation detected in Ref. [18] has multipolarity $E1$, $M1$, or $E2$, the spin is tentatively constrained to be $J^\pi = (5/2^-, 7/2 - 11/2, 13/2^-)$ by angular-momentum selection rules. Based on the low proton branching the $J^\pi = 5/2^-$ assignment seems unlikely. This level could be the mirror of the $J^\pi = 11/2^-$, 7860-keV level or the $J^\pi = (7/2, 9/2)^-$, 7736-keV level in ^{31}P. For the rate calculation we arbitrarily choose the $J^\pi = 11/2^-$ level.

7699, 7725, and 7744 keV. A 7725-keV level has been identified as a multiplet by Vernotte *et al.* [35] who observed a broad (^{3}He, α) peak with an angular distribution that was not fit well using the DWBA with a single value of ℓ_n for the transferred neutron. We measured three levels at 7699(3), 7723(3), and 7744(3) keV.

The isotropic fit to the 7699-keV angular correlation yielded a p value of 0.012, resulting in $\ell_{\min} = 1$ (Fig. 6), which constrains its spin to be $J^\pi = (1/2^- - 13/2^-)$. If we tentatively identify it with the 7707(8)*-keV level deduced from ^{31}Cl β^+-decay work [16,37], this further constrains its spin to be $J^\pi = (1/2^+, 3/2^+, 5/2^+)^*$, resulting in a final assignment of $J^\pi = (5/2^+)$.

The central level at 7725 keV was observed to have a $0.48^{+0.10}_{-0.34}$ $p_{1,2}$ branch and this is consistent with the $J^\pi = 1/2^-$ assignment made by Vernotte *et al.* [35] since the $\ell = 1$, p_1 decay of a $J^\pi = 1/2^-$ level to the 677 keV, $J^\pi = 0^+$ ^{30}P level might be competitive with the $\ell = 1$, p_0 decay to the $J^\pi = 1^+$ ground state. This lends some support to the previous identification of the 7725-keV level with the 7897 keV, $J^\pi = 1/2^-$ ^{31}P level [35], which we adopt.

The 7744-keV level has not been previously observed. For this level we constrain the spin to be $J^\pi \geqslant 5/2^+$ since the $n \leqslant 2$ fit yields a p value <0.0001, and the $n \leqslant 4$ fit is much better (Fig. 6), yielding $\ell_{\min} = 2$. Therefore we pair it with the 7736-keV ^{31}P level, which has $J^\pi = (7/2, 9/2)^-$, for the rate calculation and arbitrarily choose $7/2^-$.

7774, 7824, and 7859 keV. These three levels were measured in the vicinity of the tentatively known level at [7768(25)] keV and the known level at 7850(25) keV [14,45]. All three were measured to have a strong p_0 branch without discernible anisotropy in the angular correlation, indicating $J^\pi = (1/2^+ - 13/2^-)$. The 7824-keV level has not been previously observed.

We pair these levels with the 7825-, 7913-, and 7994-keV ^{31}P levels, respectively, for the rate calculation. Since there is no experimental information on the spin of the 7825-keV ^{31}P level, and the $1/2^+_8$ shell-model level [24,35] expected at 8189 keV is unpaired, we assume $J^\pi = 1/2^+$ for the 7774-keV ^{31}S level. The 7913-keV ^{31}P level is known to have $J^\pi = (7/2, 9/2)^-$; from this information we arbitrarily choose $J^\pi = 7/2^-$ for the 7824-keV ^{31}S level. The 7994-keV ^{31}P level is known to have $J^\pi = (1/2 - 5/2)^-$; from this information we arbitrarily choose $J^\pi = 3/2^-$ for the 7859-keV ^{31}S level.

7894 keV. Our observation of a p_0- and $p_{1,2}$-decaying level at 7894(3) keV confirms the existence of the tentatively known level [14,45] at [7888(25)] keV and suggests $J^\pi = (1/2^+ - 13/2^-)$. A 7882(15)*-keV, $J^\pi = (1/2^+, 3/2^+, 5/2^+)^*$ level was derived from ^{31}Cl β^+-decay data [16,37] and identifying the level in our measurement with this one yields $J^\pi = (1/2^+, 3/2^+, 5/2^+)$. The $J^\pi = 3/2^+$ level at 7946 keV in ^{31}P is the only mirror level known to have positive parity in this energy region so we adopt $J^\pi = 3/2^+$ for the rate calculation. Alternatively, this level could be identified with the 7912(5) keV, $J^\pi = 1/2^+$ ^{31}S level observed in (p, d) studies [19] but the energies are not in very good agreement.

7905 keV. The weak proton branching from this new level suggests that it likely has high spin. It may be the mirror analog of the $J^\pi = 11/2^-$ ^{31}P level at 8077 keV and we assume $J^\pi = 11/2^-$ for the rate calculation. The weak proton branch also indicates that it should not be identified with the 7912(5) keV, $J^\pi = 1/2^+$ ^{31}S level observed in (p, d) studies [19], which we would expect to have a dominant $\ell = 0$, p_0 decay.

7932 and 7945 keV. These levels have not been previously observed. We measure strong $\ell_{\min} = 0$ proton-decay branches from both (Fig. 6), and those constrain $J^\pi = (1/2^+ - 13/2^-)$. Using those constraints, we assume that the 7932-keV level is the mirror partner of the $J^\pi = 3/2^-$ ^{31}P level at 8049 keV for the rate calculation and adopt this spin. We identify the 7045-keV level with the tentatively observed ^{31}P level at [8085] keV with unknown spin, and arbitrarily choose $J^\pi = 7/2^+$ for the rate calculation. If the constant-width assumption used in the fits is relaxed, then it is conceivable that the 7932- and 7945-keV levels could be the same level.

7973 keV. The anomalously large $p_{1,2}$ branch of this level is suggestive of unique structure. Based on the $T = 3/2$ level energies in ^{31}Si [14], we expect the 3rd $T = 3/2$ ($J^\pi = 5/2^+$) to lie ≈1695 keV above the 1st $T = 3/2$ level, so we would expect to find it near $6281 + 1695 \approx 7980$ keV in ^{31}S. We expect the 3rd $T = 3/2$ level to have a significant isospin-permitted proton-decay branch to the $T = 1$ 1st-excited state of ^{30}P, as this level does. In addition, a level at this energy [$E_x = 7985(25)$ keV] has only been previously observed using the (^{3}He, n) reaction [45] and the excitation of $T = 3/2$ levels is also isospin permitted in that reaction. For these reasons, the 7973-keV level is a strong candidate for the 3rd $T = 3/2$ level. For the rate calculation we identify it with the 8032-keV level in ^{31}P, which is also a $J^\pi = 5/2^+$, $T = 3/2$ candidate [14].

8015, [8030], 8045, [8060], and 8071 keV levels. These levels comprise an intense, broad, and irregular peak in each of the triton singles spectra centered at ≈8045 keV. Using unconstrained widths for the fit peaks, at least 3 levels are required to obtain a satisfactory overall fit to this peak because of its irregular shape. In the p_0 triton-coincidence spectrum, there is clearly an isolated level at 8071(3) keV. In the $p_{1,2}$ spectrum there is clearly a level at 8015(3) keV. Both

coincidence spectra indicate the existence of a central level at 8044(3) keV. When we adopt these level energies and assume that all experimental widths Γ are much smaller than the instrumental width of $\approx$25 keV, two additional peaks at [8030(3)] and [8060(3)] keV are required to provide good fits of the triton-singles spectra. We classify these as tentative new levels because they are based on the constant-width assumption. All of these levels, (except the [8060]-keV level) are observed to have a significant p_0 branch under the constant-width assumption, suggesting $J^\pi = (1/2^+ - 13/2^-)$. Based on its unobserved proton branch, it is likely that the [8060]-keV level has high spin. Because of the large $p_{1,2}$ branches of the 8015- and 8045-keV levels (and their proximity to the expected energy of $\approx$7980 keV), they could be considered to be additional (weaker) candidates for the third $T = 3/2$ level. We match the 8015-keV level with the 8105-keV level in ^{31}P for the rate calculation because it is a $T = 3/2$ candidate [14], and with the 8021(16)*-keV level in ^{31}S deduced in Ref. [16], which constrains $J^\pi = (1/2^+, 3/2^+, 5/2^+)^*$. The angular distribution of a broad deuteron peak centered at 8049 keV in (p, d) studies was determined [19] to have $\ell_n = 0, 2$, and this puts a further constraint of $J^\pi = (1/2, 3/2, 5/2)^+$ on the spin of the 8045-keV level. This identification should exclude the $T = 3/2$ candidacy of the 8045-keV level since population of such a level should be isospin suppressed in the (p, d) reaction. We assume that it is the mirror partner of the $J^\pi = 3/2^+$ ^{31}P level at 8208 keV for the rate calculation. Of all levels observed in the present work, the 8045-keV level was the only level with sufficiently high statistics to extract a meaningful $p_{1,2}$ angular correlation [that was nevertheless consistent with isotropy (Fig. 6)]. Because the [8060]-keV level likely has high spin, we identify it with the $J^\pi = 11/2^+$ ^{31}P level at 8344 keV for the rate calculation. Based on consistency of the spin constraints and similar energies, we assume that the [8030]- and 8071-keV levels are paired with the 8243 keV, $J^\pi = 5/2^-$ and 8247 keV, $J^\pi = 3/2^-$ ^{31}P levels, respectively, for the rate calculation.

[8106] keV. Under the constant-width assumption, a new level at this energy was required to fit the overpopulated trough between the 8071- and 8131-keV levels in fits of the singles spectra. In addition, there is a low probability that the coincidences in this portion of the spectrum are accidental, or from the tails of intrinsically narrow, neighboring levels. This evidence tentatively supports the existence of a distinct level around this energy with $J^\pi = (1/2^+ - 13/2^-)$ that we pair with the $J = 7/2$, 8225 keV ^{31}P level for the rate calculation and arbitrarily choose positive parity. A relatively large uncertainty of 10 keV is assigned to the excitation energy of this potential level because it lies in a trough (this makes it difficult to determine the centroid), and is only statistically significant in the high-statistics spectra.

8131 keV. The isotropic fit of the $t - p_0$ angular correlation of this new level yields a p value <0.0001 and this firmly requires $J^\pi \geqslant 1/2^-$. The excellent $n \leqslant 2$ fit for this high-statistics case is somewhat suggestive of a $J^\pi = (1/2, 3/2, 5/2)^-$ assignment (Fig. 6). Therefore we pair this level with the $J^\pi = 5/2^-$, 8356 keV ^{31}P level for the rate calculation.

8178 keV. The isotropic and $n \leqslant 2$ angular-correlation hypotheses for this level are ruled out by p values of 0.0002 and 0.029, respectively (Fig. 6); this yields $\ell_{\min} = 1$ and constrains $J^\pi = (5/2^+ - 13/2^-)$. Using this constraint, we identify it with the $J^\pi = 7/2^-$, 8434-keV ^{31}P level for the rate calculation.

[8209] keV. The unobserved p_0 proton branching from this new level suggests that it has high spin. Therefore, we match it with the $J^\pi = 11/2^-$, 8414 keV ^{31}P level for the rate calculation. This level was only observed in the high-statistics spectra at low angles, and was measured to have a $p_{1,2}$ branch that was only marginally significant statistically. Therefore we classify its existence as tentative.

8229 keV. This new level was observed to have a significant $\ell_{\min} = 0$ p_0 branch (Fig. 6) and this constrains $J^\pi = (1/2^+ - 13/2^-)$. A significant $p_{1,2}$ branch was also observed. We match it with the $J^\pi = 5/2^+$, 8461-keV ^{31}P level for the rate calculation.

8273 keV. The existence of a level at 8296(21)* keV with $J^\pi = (1/2^+, 3/2^+, 5/2^+)^*$ has been inferred from ^{31}Cl β^+-delayed proton-decay studies [16,37]. We observe a level at 8268(10) keV that is consistent in energy. A relatively large excitation-energy uncertainty was assigned because the energy for this level was extracted from an extrapolation of the focal-plane calibration for the 20-MeV measurements. We tentatively identify this level with the one from the β^+-decay work, but exclude it from the rate calculation because the p_0 branching-ratio measurement is consistent with both zero and one.

8330 and 8379 keV. The 8330-keV level has not been previously observed. Both of these levels exhibited a small, but significant, $p_{1,2}$ branch with the majority of the remaining branching to the ^{30}P ground state; this constrains $J^\pi = (1/2^+ - 13/2^-)$. Using this information, we assume that these levels are paired with the 8552 keV, $J^\pi = 1/2^+$ and 8555 keV, $J^\pi = 3/2^+$ ^{31}P levels, respectively, for the rate calculation. The excitation-energy uncertainties were inflated because an extrapolation of the energy calibration for the 20-MeV measurements was used.

Above the excitation energy of 8400 keV, we do not consider any more resonances in our rate calculation because our coincidence measurements end here, and it is clear upon comparison with the level scheme of ^{31}P that the density of experimentally observed ^{31}S states is much lower than the true density of states above 8.4 MeV.

8418, 8501, 8669, 8816, and 8971 keV. Levels at 8418(21)*, 8509(16)*, [8669(40)]*, [8821(40)]*, and [8977(40)]* keV were inferred from ^{31}Cl β^+-delayed proton-decay studies [16,37], and they were assigned $J^\pi = (1/2^+, 3/2^+, 5/2^+)^*$. We observed levels at 8418(5), 8498(5), 8813(15), and 8969(20); we tentatively identify these with the 8418(21)*, 8509(16)*, [8821(40)]*, and [8977(40)]* keV levels, respectively. This supports the existence of the latter two and suggests $J^\pi = (1/2^+, 3/2^+, 5/2^+)^*$ for these four levels. In addition a ^{31}S level at 8517(13) keV was observed in (p, d) studies [19] and assigned $J^\pi = 1/2^+$ based on the $\ell_n = 0$ angular distribution; we identify this level with the 8498(5) keV level observed in the present work based on the nearly consistent excitation energies. The level at [8669(40)]* keV

was not observed in the present work. The excitation-energy uncertainties of levels were gradually inflated from 5 keV at $E_x \approx 8.5$ MeV with increasing excitation energy because unpublished data [29–31] were used to calibrate this portion of the focal plane.

8461 keV. This level has been assigned $J^\pi = (13/2)^-$ in previous work [17] and is not observed in the present study. The uncertainty in the energy of this level was not reported, but is likely ≈2 keV or less based on typical γ-ray uncertainties reported in that work.

8562, 8904, 9004, 9077, 9154, 9190, 9206, 9226, 9332, and 9422 keV. These levels were observed in our 25-MeV singles spectra only, which extended to higher excitation energies than the 20-MeV spectra. The presently observed 9190(25)- and 9398(30)-keV levels are tentatively identified with the 9207(5)- and 9423(7)-keV ^{31}S levels observed in a recent (p, d) study [19], respectively, based on similar excitation energies. We identify the presently observed 9151(25)-keV level with the previously observed 9154.0(12)-keV ^{31}S level [17] based on similar excitation energies. The other levels have not been previously observed. Our measurements did not extend above the excitation energy of 9.4 MeV. However, it should be noted that a 10146-keV ^{31}S level was tentatively assigned $J^\pi = (13/2)^-$ in previous work [17,19], but the assignment has recently been firmly determined to be $J^\pi = 15/2^-$ [39].

[1] J. José, A. Coc, and M. Hernanz, Astrophys. J. **560**, 897 (2001).
[2] C. Iliadis, J. M. D'Auria, S. Starrfield, W. J. Thompson, and M. Wiescher, Astrophys. J. Suppl. Ser. **134**, 151 (2001).
[3] J. José and M. Hernanz, J. Phys. G **34**, 431 (2007).
[4] S. Amari, X. Gao, L. R. Nittler, E. Zinner, J. José, M. Hernanz, and R. S. Lewis, Astrophys. J. **551**, 1065 (2001).
[5] J. José, M. Hernanz, S. Amari, K. Lodders, and E. Zinner, Astrophys. J. **612**, 414 (2004).
[6] L. R. Nittler and P. Hoppe, Astrophys. J. **631**, L89 (2005).
[7] A. Chieffi, M. Limongi, and O. Straniero, Astrophys. J. **502**, 737 (1998).
[8] C. Iliadis, *Nuclear Physics of Stars* (Wiley-VCH, Weinheim, 2007).
[9] W. Hauser and H. Feshbach, Phys. Rev. **87**, 366 (1952).
[10] G. R. Caughlan and W. A. Fowler, At. Data Nucl. Data Tables **40**, 283 (1988).
[11] F.-K. Thielemann, M. Arnould, and J. W. Truran, in *Advances in Nuclear Astrophysics: Proceedings of the Second IAP Workshop, Paris, France, 1986*, edited by E. Vangioni-Flam *et al.* (Editions Frontières, Gif-sur-Yvette, 1986), p. 525.
[12] T. Rauscher and F.-K. Thielemann, At. Data Nucl. Data Tables **79**, 47 (2001).
[13] G. Audi, A. H. Wapstra, and C. Thibault, Nucl. Phys. **A729**, 337 (2003).
[14] P. M. Endt, Nucl. Phys. **A521**, 1 (1990).
[15] P. M. Endt, Nucl. Phys. **A633**, 1 (1998).
[16] A. Kankainen, T. Eronen, S. P. Fox, H. O. U. Fynbo, U. Hager, J. Hakala, J. Huikari, D. G. Jenkins, A. Jokinen, S. Kopecky *et al.*, Eur. Phys. J. A **27**, 67 (2006).
[17] D. G. Jenkins, C. J. Lister, M. P. Carpenter, P. Chowdhury, N. J. Hammond, R. V. F. Janssens, T. L. Khoo, T. Lauritsen, D. Seweryniak, T. Davinson *et al.*, Phys. Rev. C **72**, 031303(R) (2005).
[18] D. G. Jenkins, A. Meadowcroft, C. J. Lister, M. P. Carpenter, P. Chowdhury, N. J. Hammond, R. V. F. Janssens, T. L. Khoo, T. Lauritsen, D. Seweryniak *et al.*, Phys. Rev. C **73**, 065802 (2006).
[19] Z. Ma, D. W. Bardayan, J. C. Blackmon, R. P. Fitzgerald, M. W. Guidry, W. R. Hix, K. L. Jones, R. L. Kozub, R. J. Livesay, M. S. Smith *et al.*, Phys. Rev. C **76**, 015803 (2007).
[20] C. Wrede, J. A. Caggiano, J. A. Clark, C. Deibel, A. Parikh, and P. D. Parker, Phys. Rev. C **76**, 052802(R) (2007).
[21] A. Parikh, Ph.D. thesis (Yale University, 2006).
[22] D. W. Visser, Ph.D. thesis (Yale University, 2003).
[23] H.-S. Tzeng, J.-Y. Liu, I. Sugai, and Y. C. Liu, Nucl. Instrum. Methods Phys. Res. **150**, 143 (1978).
[24] B. H. Wildenthal, Prog. Part. Nucl. Phys. **11**, 5 (1984).
[25] C. Wrede, Ph.D. thesis (Yale University, 2008).
[26] T. Davinson, W. Bradfield-Smith, S. Cherubini, A. DiPietro, W. Galster, A. M. Laird, P. Leleux, A. Ninane, A. N. Ostrowski, A. C. Shotter *et al.*, Nucl. Instrum. Methods Phys. Res. A **454**, 350 (2000).
[27] W. Bradfield-Smith, R. Lewis, P. D. Parker, and D. W. Visser, Nucl. Instrum. Methods Phys. Res. A **481**, 183 (2002).
[28] K. B. Swartz, D. W. Visser, and J. M. Baris, Nucl. Instrum. Methods Phys. Res. A **463**, 354 (2001); http://jam-daq.wiki.sourceforge.
[29] C. M. Deibel, Ph.D. thesis (Yale University, 2008).
[30] C. M. Deibel (private communication).
[31] R. Lewis, Ph.D. thesis (Yale University, 2005).
[32] A. H. Wapstra, G. Audi, and C. Thibault, Nucl. Phys. **A729**, 129 (2003).
[33] A. J. Ferguson, *Angular Correlation Methods in Gamma-ray Spectroscopy* (Wiley, New York, 1965).
[34] J. W. Noé, D. P. Balamuth, and R. W. Zurmühle, Phys. Rev. C **9**, 132 (1974).
[35] J. Vernotte, G. Berrier-Ronsin, S. Fortier, E. Hourani, A. Khendriche, J. M. Maison, L.-H. Rosier, G. Rotbard, E. Caurier, and F. Nowacki, Nucl. Phys. **A655**, 415 (1999).
[36] P. M. Endt and C. van der Leun, Nucl. Phys. **A310**, 1 (1978).
[37] J. Aysto, X. J. Xu, D. M. Moltz, J. E. Reiff, J. Cerny, and B. H. Wildenthal, Phys. Rev. C **32**, 1700 (1985).
[38] F. Della Vedova, S. M. Lenzi, M. Ionescu-Bujor, N. Mărginean, M. Axiotis, D. Bazzacco, A. M. Bizzeti-Sona, P. G. Bizzeti, A. Bracco, F. Brandolini *et al.*, Phys. Rev. C **75**, 034317 (2007).
[39] M. Ionescu-Bujor, A. Iordachescu, D. R. Napoli, S. M. Lenzi, N. Mărginean, T. Otsuka, Y. Utsuno, R. V. Ribas, M. Axiotis, D. Bazzacco *et al.*, Phys. Rev. C **73**, 024310 (2006).
[40] A. R. Barnett, Comput. Phys. Commun. **27**, 147 (1982).
[41] C. Iliadis, Nucl. Phys. **A618**, 166 (1997).
[42] D. A. Hutcheon *et al.*, TRIUMF EEC proposal E1108 (unpublished).
[43] F. Della Vedova (private communication).
[44] A. Parikh (private communication).

[45] J. M. Davidson, D. A. Hutcheon, D. R. Gill, T. Taylor, D. M. Sheppard, and W. C. Olsen, Nucl. Phys. **A240**, 253 (1975).
[46] J. F. Wilkerson, R. E. Anderson, T. B. Clegg, E. J. Ludwig, and W. J. Thompson, Phys. Rev. Lett. **51**, 2269 (1983).
[47] E. G. Adelberger, A. B. McDonald, C. L. Cocke, C. N. Davids, A. P. Shukla, H. B. Mak, and D. Ashery, Phys. Rev. C **7**, 889 (1973).
[48] H. A. Enge, Nucl. Instrum. Methods Phys. Res. **162**, 161 (1979).